

Interpreting the Low Frequency Radio Spectra of Starburst Galaxies: A Pudding of Strömgren Spheres

Brian C. Lacki^{1,2}

¹*Jansky Fellow of the National Radio Astronomy Observatory*

²*Institute for Advanced Study, Einstein Drive, Princeton, NJ 08540, USA, brianlacki@ias.edu*

Draft Version

ABSTRACT

The low frequency radio emission of starburst galaxies is informative, but it can be absorbed in several ways. Most importantly, starburst galaxies are home to many H II regions, whose free-free absorption can obscure low frequency radio waves. These H II regions are discrete objects, but most multiwavelength models of starbursts assume a uniform medium of ionized gas, if they include the absorption at all. I calculate the effective absorption coefficient of H II regions in starbursts, which is ultimately a cross section times the density of H II regions. The cross section can be easily calculated by assuming that H II regions are Strömgren spheres. The coefficient asymptotes to a constant value at low frequencies, because H II regions partially cover the starburst, and are buried part way into the starburst's synchrotron emitting material. Considering Strömgren spheres around both O stars and Super Star Clusters, I apply the calculations to the low frequency radio spectrum of M82. Far from being opaque at low frequencies, I find that M82 mostly transmits its radio flux. I also find that starbursts are transparent down to a few MHz to other possible absorption processes, such as free-free absorption from the diffuse superwind phase, synchrotron self-absorption, and the Razin effect. Hence, starburst galaxies should be observable with new low frequency radio telescopes.

Key words: radio continuum: general – radio continuum: ISM – galaxies: starburst – H II regions – galaxies: individual (M82)

1 INTRODUCTION

The radio spectrum of star-forming galaxies, including starbursts, is dominated by synchrotron emission from cosmic ray (CR) electrons and positrons (e^\pm) in diffuse magnetic fields (Condon 1992). There is also free-free emission, which typically comes from H II regions in a galaxy. Both of these emission processes are associated with star-formation: cosmic rays are generated somehow by star formation (possibly through shock acceleration in supernova remnants), and H II regions surround young, massive stars that produce ionizing radiation. Since synchrotron emission has a steeply falling spectrum (typically $S_\nu^{\text{synch}} \propto \nu^{-0.7}$) whereas free-free emission does not ($S_\nu^{\text{ff}} \propto \nu^{-0.1}$), the synchrotron emission dominates below about 30 GHz (e.g., Condon 1992; Niklas, Klein, Wielebinski 1997).

There is a wealth of information available at MHz frequencies. In particular, different cooling processes may set the CR e^\pm lifetime at different energies. At low frequencies, bremsstrahlung, with an energy-independent loss time, and ionization, which is most effective at low energies, become more important than synchrotron and

Inverse Compton cooling, which grow stronger at high energies (Hummel 1991; Thompson et al. 2006; Murphy 2009; Lacki, Thompson, & Quataert 2010). Any escape, whether diffusive or advective, also becomes more important relative to synchrotron at low frequencies. Therefore, the synchrotron radio spectrum should flatten at low frequencies and steepen at high frequencies. Indeed, this behaviour is often seen in the radio spectra of starburst galaxies (e.g., Clemens et al. 2008; Williams & Bower 2010; Leroy et al. 2011). The detailed radio spectra is then useful in constructing models of the cosmic ray population, helping to constrain the poorly understood magnetic field strength (e.g., Torres 2004; Domingo-Santamaría & Torres 2005; Persic, Rephaeli, & Arieli 2008; de Cea del Pozo, Torres, & Rodríguez Marrero 2009; Lacki et al. 2010; Rephaeli, Arieli, & Persic 2010; Crocker et al. 2011). Low frequency synchrotron emission might also reveal the presence of a ‘pion bump’ in the e^\pm spectrum, in which the spectrum of secondary e^\pm from pion decay falls off due to the kinematics of pion production in proton-proton collisions (Rengarajan 2005).

In practice, our ability to understand the low frequency

radio spectrum of starbursts is limited by other processes which alter the radio spectrum. The most important is free-free absorption by ionized gas in galaxies. The Galactic radio spectrum has a turnover at ~ 3 MHz, largely caused by free-free absorption in the diffuse Warm Ionized Medium (Alexander et al. 1969; Fleishman & Tokarev 1995; Peterson & Webber 2002). Free-free absorption is even more important along lines of sight through dense H II regions, which can become optically thick even at GHz frequencies (e.g., McDonald et al. 2002). Free-free absorption, like ionization and bremsstrahlung cooling, can flatten the low frequency radio spectra of starbursts. The spectral curvature of starburst galaxies has therefore also been interpreted as free-free absorption (Klein, Wielebinski, & Morsi 1988; Carilli 1996; Clemens et al. 2010).

The observational prospects for low frequency studies of star-forming galaxies are good. There is increasing interest in low frequency radio observations, due to their value in observing high redshift 21 cm lines, among other reasons. The Giant Metrewave Radio Telescope (GMRT) is specifically designed to provide interferometric data for radio sources in the 50 MHz to 1.5 GHz range with high sensitivity¹. The 74 and 333 MHz systems on the Very Large Array (VLA) provide high angular resolution images (Kassim et al. 2007), and have completed a survey of the northern sky (Cohen et al. 2007). It is currently being upgraded for use on the Jansky VLA. The Low Frequency Array (LOFAR), now coming online, is a new radio telescope with long baseline interferometry capabilities, and can go all the way down to 15 MHz². The Leiden LOFAR Sky Surveys Project³ will image some nearby star-forming galaxies in radio, possibly including starbursts like M82. LOFAR will be joined by the 21 cm pathfinder experiments at frequencies above 100 MHz and possibly the Long Wavelength Array at frequencies of 10 to 88 MHz (e.g., Ellingson et al. 2009). Ultimately, the Square Kilometre Array (SKA) should be able to observe galaxies down to 70 MHz with high sensitivity⁴.

However, there has been relatively little work on the theory of the low frequency radio spectra of starburst galaxies. For model fitting, the typical assumption, if free-free absorption is even considered at all, is the uniform slab model, in which both the free-free absorption and emission comes from a uniform density ionized medium pervading the synchrotron-emitting region (for examples of uniform slabs used to fit starburst radio spectra, see, e.g., Sopp & Alexander 1991; Condon et al. 1991; Carilli 1996; Torres 2004; Clemens et al. 2010; Williams & Bower 2010). The best measurements are at GHz frequencies, where the integrated free-free absorption is often expected to be small and the details of the absorption may not matter much, though it has been claimed to be important at GHz frequencies in Arp 220 and other Ultraluminous Infrared Galaxies (ULIRGs) (Condon et al. 1991; Sopp & Alexander 1991; Clemens et al. 2008, 2010). However, from a theoretical point of view, this approximation is likely to be too simple: in the Milky Way, while the free-free absorption largely

comes from the diffuse ionized medium, the free-free emission comes from compact H II regions. On the other hand, in starburst galaxies, at least part of the free-free absorption is observed to come from discrete H II regions, as seen in the Galactic Centre (Brogan et al. 2003; Nord et al. 2006), and in M82 (Wills et al. 1997). Discrete H II regions partially cover starbursts: some of the sightlines through the starburst do not intercept an H II region and are unabsorbed at any frequency.

The alternative is to consider starbursts as a collection of discrete H II regions. A simple version of this approach has been considered in the context of radio recombination line studies, where the radio spectrum is needed to calculate stimulated emission (e.g., Anantharamaiah et al. 1993; Zhao et al. 1996; Rodríguez-Rico et al. 2005). The typical assumption in these models is that all of the H II regions have the same density, temperature, and radius, and are located in the midplane of a starburst disc. Each H II region then shadows the synchrotron-emitting region behind it: with this assumption, the free-free absorption can be predicted (e.g., Anantharamaiah et al. 1993). However, the model does not work well when the H II regions are both optically thick and have a covering fraction near 100% (Anantharamaiah et al. 1993), and it does not allow for H II regions of different radii.

In this paper, I study effects on the low frequency spectra of starbursts. I focus on free-free absorption, the most important process. I calculate the amount of free-free absorption by assuming it comes from discrete H II regions around stellar clusters in starbursts. In essence, I treat a starburst as a pudding with Strömgren spheres mixed in. My model generalizes the approach of Anantharamaiah et al. (1993) to allow H II regions of different radii, here assumed to correspond to young star clusters of different masses, and allows for optically thick H II regions with high covering fraction. I make spectral fits using these model to the low frequency radio spectrum of M82 in Section 4, accounting for the possibility of spectral curvature. I also consider whether other processes, such as free-free absorption from the keV plasma of the starburst wind, the Razin effect, or synchrotron self-absorption, could cut off the low frequency spectrum in Section 5.

2 A METHOD FOR CALCULATING FREE-FREE ABSORPTION FROM DISCRETE H II REGIONS

The nonthermal continuum radio emission of starbursts are thought to pervade the entire starburst region, because the radiating cosmic rays can diffuse from their acceleration sites (e.g., Torres et al. 2012). The H II regions are intermixed in the starburst region, so in this sense the uniform slab model is correct. However, a model of truly uniform ionized gas assumes the free-free absorption comes from a low density, high filling factor medium, which would have a low turnover frequency, but would be highly opaque below the turnover frequency. However, a more appropriate assumption is that there is a uniform density of H II regions rather than of ionized gas. A uniform collection of discrete H II regions is a high density, low filling factor medium, with a

¹ See <http://www.gmrt.ncra.tifr.res.in>.

² At <http://www.lofar.org>.

³ With a home page at <http://lofar.strw.leidenuniv.nl/>.

⁴ <http://www.skatelescope.org>.

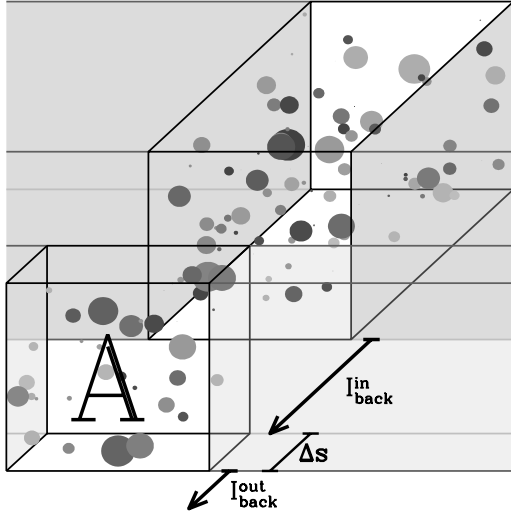


Figure 1. H II regions (filled circles) in a slice of the starburst with area A and thickness Δs absorb radiation from the column behind it. The column can be small relative to the rest of the starburst (shaded in grey), but each slice is large enough to contain a representative sample of H II regions. A beam of light is emitted from the background column, enters perpendicular to the slice with intensity $I_{\text{back}}^{\text{in}}$ and emerges with intensity $I_{\text{back}}^{\text{out}}$, where I is flux per solid angle. The fraction of light absorbed passing through the slice, which can be calculated by summing over individual H II regions in the slice, is directly related to the mean effective absorption coefficient of the starburst from H II regions. The coefficient then can be used in a uniform slab model (as suggested by the uniform grey shading of the rest of the starburst).

higher turnover frequency, but also translucent below that frequency.

2.1 Derivation of Absorption Coefficient for Discrete H II Regions

I start by considering how a thin slice of the starburst with thickness Δs absorbs background radio emission passing perpendicularly through it (Figure 1). The slice has an area A and thickness large enough to contain a representative sample of the starburst's H II regions, but otherwise can be small compared to the starburst. I ignore the H II regions' effects on radio emission emitted within the slice – as long as the slice is thin, and as long as the H II regions have a small filling factor, this should be a valid approximation. If the filling factor is large, a true uniform slab model is more accurate anyway.

Suppose that there are M H II regions (indexed by the number m). Each H II region passes a fraction Φ_m of the normal incident radiation $I_{\text{back}}^{\text{in}} A$ on the slice, where I is flux per solid angle. For example, if a totally opaque sphere of radius r sat in a slice of area A , $\Phi = 1 - (\pi r^2/A)$. Then the background radio intensity after passing through the slice is

$$I_{\text{back}}^{\text{in}} A \left[\prod_{m=1}^M \Phi_m \right] = I_{\text{back}}^{\text{out}} A. \quad (1)$$

Taking the logarithm of both sides, we can rephrase this as an optical depth:

$$-\sum_{m=1}^M \ln \Phi_m = -\ln \left(\frac{I_{\text{back}}^{\text{out}}}{I_{\text{back}}^{\text{in}}} \right) \equiv \Delta\tau_{\text{eff}}. \quad (2)$$

Because each H II fraction only covers a small portion of the starburst, a convenient approximation is to define $\phi_m = 1 - \Phi_m$ and then to assume that $\ln \Phi_m \approx -\phi_m$. This is equivalent to saying that the H II regions do not overlap within the slice. Then we have

$$\sum_{m=1}^M \phi_m \approx \Delta\tau_{\text{eff}}. \quad (3)$$

If there are J types of H II regions, where each type of H II region absorbs the same amount of background radio, and if there are K_j H II regions of each type j within the slice, then

$$\Delta\tau_{\text{eff}} \approx \sum_{j=1}^J K_j \phi_j. \quad (4)$$

More realistically, instead of having a few distinct types of H II regions, there will be a distribution function parametrizing the absorption properties of H II regions. Suppose the number of H II regions with some relevant physical quantity (such as radius) between q and $q + dq$ and within a volume dV is $dN/(dq dV)$. Then, since the volume of the slice is $A\Delta s$, the effective optical depth is

$$\Delta\tau_{\text{eff}} \approx \int \frac{dN}{dq dV} (A\Delta s) \phi(q) dq. \quad (5)$$

Of course, this can easily be generalized to more than one parameter.

The effective optical depth across the slice translates to an effective absorption coefficient $\alpha_{\text{eff}} \equiv \Delta\tau_{\text{eff}}/(\Delta s)$ of the starburst. Furthermore, the quantity $A\phi(q)$ is an effective absorption cross section σ for each H II region. So we have

$$\alpha_{\text{eff}} \approx \int \frac{dN}{dq dV} \sigma(q) dq. \quad (6)$$

Therefore, the absorption coefficient reduces to a number density times a cross section, as might be expected.

If the density of H II regions is constant throughout the starburst, the equation of radiative transfer through the starburst,

$$\frac{dI}{ds} \approx -\alpha_{\text{eff}} I + j \quad (7)$$

has the uniform slab solution:

$$I = \frac{j}{\alpha_{\text{eff}}} (1 - e^{-\tau_{\text{eff}}}) \quad (8)$$

except that the optical depth is the effective optical depth defined as $\tau_{\text{eff}} = \alpha_{\text{eff}} s$, where s is the sightline length through the starburst. Of course, the density of H II regions may itself vary, for example, decreasing towards the edge of the starburst. However, the basic principle remains the same: the effective absorption coefficient is calculated at each point using equation 6, and then used in the radiative transfer equation to find the synchrotron intensity on each sightline.

2.1.1 The effective cross section for translucent spheres

I treat H II regions as Strömgren spheres, which free-free absorb the radiation behind them. The effective cross section of a sphere of radius R_S and absorption coefficient α_{HII} is equal to the projected area of the H II region times the fraction of background flux it obscures:

$$\sigma = \int_0^{R_S} 2\pi y \left[1 - e^{-2\alpha_{\text{HII}} \sqrt{R_S^2 - y^2}} \right] dy \quad (9)$$

$$= \pi R_S^2 - \frac{\pi}{2\alpha_{\text{HII}}} \left[1 - e^{-2\alpha_{\text{HII}} R_S} (1 + 2\alpha_{\text{HII}} R_S) \right] \quad (10)$$

When α_{HII} is very large (at low frequency, for example), the spheres become totally opaque and the effective cross section is just πR_S^2 . If instead α_{HII} is very small, as at high frequency, the effective cross section goes as $(4/3)\pi\alpha_{\text{HII}}R_S^3$.

A simpler approximation, the blue edge approximation, for the effective absorption cross section of the sphere assumes it is completely transparent when $\tau_{\text{HII}} \approx \alpha_{\text{HII}}R_S < 1$ and completely opaque when $\tau_{\text{HII}} > 1$:

$$\sigma \approx \begin{cases} \pi R_S^2 & (\alpha_{\text{HII}}R_S > 1) \\ 0 & (\alpha_{\text{HII}}R_S < 1) \end{cases} \quad (11)$$

This approximation works well at high and low frequencies, but at intermediate frequencies, it can fail.

2.1.2 The covering fraction

The calculation of the covering fraction of the H II regions is analogous to the calculation of the absorption of the radio flux. Essentially, we are interested in how much of the background sky is blocked by the H II regions. We can phrase this in terms of a flux calculation: if H II regions are totally opaque, the covering fraction is equal to the fraction of a uniform background intensity they absorb. Thus, we have for a distribution function of H II regions

$$\alpha_{\text{cover}} = \int \frac{dN}{dq dV} \pi R_S^2 dq. \quad (12)$$

For the covering fraction calculation, the H II regions are treated as a foreground screen rather than as a uniform slab, as it does not matter how deep into the starburst any H II region is. From the solution to absorption from a foreground screen, the probability any given sightline is covered is

$$P_{\text{cover}} = 1 - e^{-\alpha_{\text{cover}} s}, \quad (13)$$

where s is the length of the sightline, assuming α_{cover} is uniform throughout the starburst.

The length of a sightline may vary; for example, in an edge-on disc, it is shorter towards the rim than through the centre. The covering fraction for the entire starburst is the average of the covering probability P_{cover} over all sightlines that pass through the starburst:

$$f_{\text{cover}} = \frac{1}{\Omega_{\text{obs}}} \int (1 - e^{-\alpha_{\text{cover}} s}) d\Omega_{\text{obs}}. \quad (14)$$

In this equation, Ω_{obs} is the solid angle subtended by the entire starburst from Earth. Note that since starbursts are small on the sky, Ω_{obs} is directly proportional to the projected area of the starburst A_{proj} :

$$f_{\text{cover}} = \frac{1}{A_{\text{proj}}} \int (1 - e^{-\alpha_{\text{cover}} s}) dA_{\text{proj}}. \quad (15)$$

A natural consequence of $f_{\text{cover}} < 1$ is that we expect the optical depth to increase to some maximum value at low frequency and no further. If there are just a few H II regions, then the covering fraction is small and parts of the starburst remain completely unobscured. However, even if the density of H II regions is high, discrete H II regions tend to overlap from our point of view and cover each other instead of background material. This leads to a covering fraction less than 1. Thus, unlike a diffuse ionized medium, discrete H II regions lead to non-zero radio emission at low frequencies.

2.1.3 The filling fraction

Likewise, we can calculate the filling fraction from a distribution of Strömgren spheres. The starburst has a volume V_{SB} , and a Strömgren sphere of radius R_S has volume $4/3\pi R_S^3$. Therefore, each sphere leaves a fraction $1 - 4\pi R_S^3/(3V)$ of the starburst unfilled, and the filling factor can be calculated using

$$1 - f_{\text{fill}} \approx \exp \left[- \int \frac{dN}{dq} \left(\frac{4\pi R_S(q)^3}{3V_{\text{SB}}} \right) dq \right]. \quad (16)$$

When the filling factor is small, the spheres do not overlap, and

$$f_{\text{fill}} \approx \int \frac{dN}{dq} \left(\frac{4\pi R_S(q)^3}{3V_{\text{SB}}} \right) dq. \quad (17)$$

Since R_S is much smaller than the size of the starburst, the filling factor of H II regions can be much smaller than 1 even if the covering fraction is nearly 1. As a result, a sightline through the starburst will not immediately intercept an H II region, even if the covering fraction is nearly 1. Instead, the first absorbing H II region on the sightline is buried past unobscured synchrotron-emitting space: this ensures that there is still synchrotron radio flux at low frequencies even if the covering fraction is high.

2.2 Using the absorption to calculate integrated flux

The uniform slab solution provides the intensity along a single sightline, which can be appropriate if the starburst is resolved. However, we often are interested in the integrated flux of the starburst. The sightline will have different lengths as it passes through different parts of the starburst. I derive for the reader how much integrated flux remains after free-free absorption for three common geometries: a disc viewed face-on, a disc viewed edge-on, and a sphere.

2.2.1 A face-on disc

The flux observed at Earth is proportional to the luminosity emitted by the starburst into a unit solid angle, $dL/d\Omega_{\text{em}} = \int I dA_{\text{proj}}$. For a face-on disc of radius R_{SB} and midplane-to-edge height h_{SB} (edge-to-edge height $2h_{\text{SB}}$), this is simply $dL/d\Omega_{\text{em}} = \pi R_{\text{SB}}^2 I$, or

$$\frac{dL}{d\Omega_{\text{em}}} = \pi R_{\text{SB}}^2 \frac{j}{\alpha_{\text{eff}}} (1 - e^{-2\alpha_{\text{eff}} h_{\text{SB}}}). \quad (18)$$

If the starburst had no absorption, it would have $dL/d\Omega_{\text{em}} = 2\pi R_{\text{SB}}^2 h_{\text{SB}} j$. Therefore, the ratio of actual flux to flux without absorption is

$$\frac{F}{F_{\text{unabs}}} = \frac{1 - e^{-2\alpha_{\text{eff}} h_{\text{SB}}}}{2\alpha_{\text{eff}} h_{\text{SB}}}, \quad (19)$$

asymptoting to $1 - \alpha_{\text{eff}} h_{\text{SB}}$ when α_{eff} is very small and the starburst is nearly transparent.

The covering fraction for this geometry is just

$$f_{\text{cover}} = 1 - e^{-2\alpha_{\text{cover}} h_{\text{SB}}}. \quad (20)$$

2.2.2 An edge-on disc

If the starburst disc is instead observed edge-on, the sightline length s through the disc varies between 0 and R_{SB} . Defining y as the impact parameter from the centre of the disc, so that $y = \sqrt{R_{\text{SB}}^2 - s^2/4}$, the emergent flux is related to

$$\begin{aligned} \frac{dL}{d\Omega_{\text{em}}} &= 2h_{\text{SB}} \times 2 \int_0^{R_{\text{SB}}} \frac{j}{\alpha_{\text{eff}}} (1 - e^{-\alpha_{\text{eff}} s}) dy \\ &= 4h_{\text{SB}} \frac{j}{\alpha_{\text{eff}}} \left(R_{\text{SB}} - \int_0^{R_{\text{SB}}} e^{-2\alpha_{\text{eff}} \sqrt{R_{\text{SB}}^2 - y^2}} dy \right) \end{aligned} \quad (21)$$

The ratio of actual flux to flux without absorption is

$$\frac{F}{F_{\text{unabs}}} = \frac{2}{\pi\alpha_{\text{eff}} R_{\text{SB}}} \left(1 - \int_0^1 e^{-2\alpha_{\text{eff}} R_{\text{SB}} \sqrt{1-u^2}} du \right). \quad (23)$$

When the disc is nearly transparent, with small α_{eff} , the ratio is approximately $1 - 8\alpha_{\text{eff}} R_{\text{SB}}/(3\pi)$.

The covering fraction is $1/(4h_{\text{SB}} R_{\text{SB}}) \int_{-R_{\text{SB}}}^{R_{\text{SB}}} \int_{-h_{\text{SB}}}^{h_{\text{SB}}} (1 - e^{-\alpha_{\text{cover}} s}) dx dy$, which simplifies to

$$f_{\text{cover}} = 1 - \int_0^1 e^{-2\alpha_{\text{cover}} R_{\text{SB}} \sqrt{1-u^2}} du. \quad (24)$$

When $\alpha_{\text{cover}} R_{\text{SB}} \ll 1$, $f_{\text{cover}} \approx (\pi/2) R_{\text{SB}} \alpha_{\text{cover}}$.

2.2.3 A sphere

Suppose instead a starburst is a sphere with radius R_{SB} . Much like the case of an edge-on disc, the sightline length s varies between 0 and R_{SB} , depending on the impact parameter y from the centre of the sphere, with $y = \sqrt{R_{\text{SB}}^2 - s^2/4}$. The emergent flux is now proportional to

$$\begin{aligned} \frac{dL}{d\Omega_{\text{em}}} &= 2\pi \int_0^{R_{\text{SB}}} y \frac{j}{\alpha_{\text{eff}}} (1 - e^{-\alpha_{\text{eff}} s}) dy \\ &= \frac{\pi j}{\alpha_{\text{eff}}} \left[R_{\text{SB}}^2 + \left(\frac{R_{\text{SB}}}{\alpha_{\text{eff}}} + \frac{1}{2\alpha_{\text{eff}}^2} \right) e^{-2\alpha_{\text{eff}} R_{\text{SB}}} - \frac{1}{2\alpha_{\text{eff}}^2} \right] \end{aligned} \quad (25)$$

In a transparent sphere, the luminosity per solid angle is $dL/d\Omega_{\text{em}} = (4/3)\pi R_{\text{SB}}^3 j$. Thus the ratio of actual flux to unabsorbed flux is

$$\frac{F}{F_{\text{unabs}}} = \frac{3}{4\alpha_{\text{eff}} R_{\text{SB}}^3} \left[R_{\text{SB}}^2 + \left(\frac{R_{\text{SB}}}{\alpha_{\text{eff}}} + \frac{1}{2\alpha_{\text{eff}}^2} \right) e^{-2\alpha_{\text{eff}} R_{\text{SB}}} - \frac{1}{2\alpha_{\text{eff}}^2} \right] \quad (26)$$

In the limit when α_{eff} is small, this ratio is $1 - (3/4)\alpha_{\text{eff}} R_{\text{SB}}$.

The equation for the covering fraction is now $f_{\text{cover}} = 1/(\pi R_{\text{SB}}^2) \int_0^{R_{\text{SB}}} 2\pi y (1 - e^{-\alpha_{\text{cover}} s}) dy$. This can be solved, giving:

$$f_{\text{cover}} = 1 + \frac{1}{2R_{\text{SB}}^2 \alpha_{\text{cover}}^2} [e^{-2\alpha_{\text{cover}} R_{\text{SB}}} (2\alpha_{\text{cover}} R_{\text{SB}} + 1) - 1]. \quad (28)$$

This reduces to $f_{\text{cover}} \approx (4/3)\alpha_{\text{cover}} R_{\text{SB}}$ when $\alpha_{\text{cover}} R_{\text{SB}} \ll 1$.

3 APPLICATION TO POPULATIONS OF H II REGIONS IN STARBURSTS

I now calculate the free-free absorbing properties of H II regions in starbursts. I assume that the ionizing sources in starbursts are either O stars or stellar clusters acting as point sources, each with an ionizing photon luminosity Q_{ion} . I then assume the H II regions are spheres with the Strömgen radius:

$$R_S = \left(\frac{3Q_{\text{ion}}}{4\pi n_H^2 \alpha_B} \right)^{1/3}. \quad (29)$$

The recombination constant α_B is equal to $\alpha_B = 2.56 \times 10^{-13} (T/10^4 \text{ K})^{-0.83} \text{ cm}^3 \text{ s}^{-1}$ (Draine 2011a).

For a long-lived ($\gtrsim 10$ Myr) continuous starburst, Leitherer et al. (1999) finds the ionizing photon luminosity as

$$Q_{\text{ion}} = 2.18 \times 10^{53} \text{ ph s}^{-1} \left(\frac{\text{SFR}}{\text{M}_{\odot} \text{ yr}^{-1}} \right), \quad (30)$$

assuming Solar metallicity and a Salpeter mass function from 0.1 to 100 M_{\odot} . I divide this ionizing luminosity into a calculated number of O stars or star clusters to find the typical ionizing luminosity of a source.

3.1 H II regions around individual O stars

One possible assumption is that the ionizing sources are individual O stars. A typical O star has an ionizing photon luminosity of $\sim 10^{49} \text{ ph s}^{-1}$. Given the total ionizing photon flux of eqn. 30, the number of ionizing O stars in the galaxy is

$$N_O = 21800 \left(\frac{\text{SFR}}{\text{M}_{\odot} \text{ yr}^{-1}} \right) \left(\frac{Q_{\text{ion}}^*}{10^{49} \text{ ph s}^{-1}} \right)^{-1}. \quad (31)$$

The Strömgen radius around each O star is

$$R_S = 0.68 \text{ pc} \left(\frac{Q_{\text{ion}}^*}{10^{49} \text{ ph s}^{-1}} \right)^{1/3} \left(\frac{n_H}{1000 \text{ cm}^{-3}} \right)^{-2/3} \quad (32)$$

for $T_e = 10^4 \text{ K}$. The free-free of a fully ionized hydrogen plasma (with $n_e = n_H$) is

$$\alpha_{\text{HII}} = 0.018 \text{ cm}^{-1} \left(\frac{n_e^2 T^{-3/2} \nu^{-2} \bar{g}_{\text{ff}}}{\text{cm}^{-6} \text{ K}^{-3/2} \text{ Hz}^{-2}} \right), \quad (33)$$

with the Gaunt factor \bar{g}_{ff} usually having a value near ~ 10 for 10^4 K plasma at MHz frequencies (Rybicki & Lightman 1979). Therefore, each H II region becomes optically thick ($\alpha_{\text{HII}} R_S = 1$) when

$$\begin{aligned} \alpha_{\text{HII}} R_S &= 615 \text{ MHz} \left(\frac{T}{10^4 \text{ K}} \right)^{-3/4} \left(\frac{n_H}{1000 \text{ cm}^{-3}} \right)^{2/3} \\ &\times \left(\frac{Q_{\text{ion}}^*}{10^{49} \text{ ph s}^{-1}} \right)^{1/6} \left(\frac{\bar{g}_{\text{ff}}}{10} \right)^{1/2} \end{aligned} \quad (34)$$

If the Strömgen spheres are in a uniform density medium, then all of the spheres are the same size, and it is straightforward to calculate the effective absorption coefficient for a starburst disc:

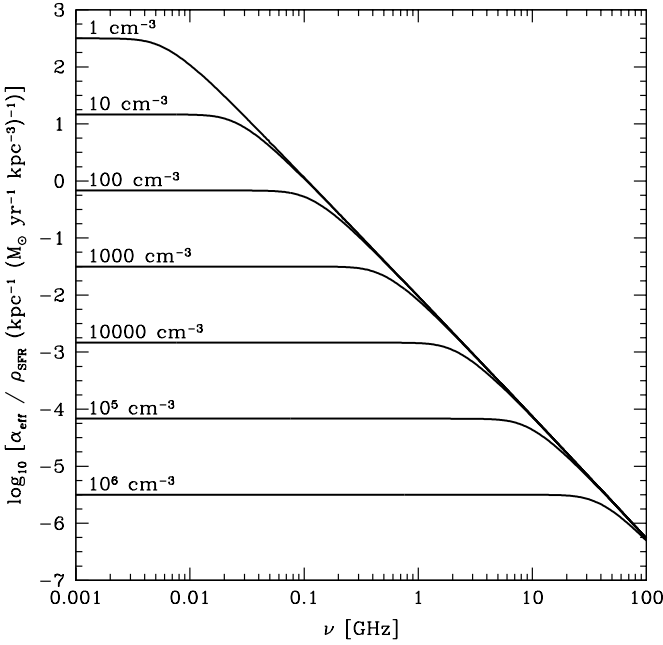


Figure 2. Effective absorption coefficient for H II regions of various densities, as normalized to a volumetric star-formation rate of $1 \text{ M}_\odot \text{ yr}^{-1} \text{ kpc}^{-3}$. This plot shows the case when each O star is single and has a Strömgren sphere around it.

$$\alpha_{\text{eff}} = \frac{N_O}{2\pi R_{\text{SB}}^2 h_{\text{SB}}} \sigma \quad (35)$$

In the blue edge approximation, the result is simple:

$$\alpha_{\text{eff}} \approx (1.2 \text{ kpc})^{-1} \left(\frac{\text{SFR}}{\text{M}_\odot \text{ yr}^{-1}} \right) \left(\frac{R_{\text{SB}}}{250 \text{ pc}} \right)^{-2} \left(\frac{h_{\text{SB}}}{100 \text{ pc}} \right)^{-1} \times \left(\frac{Q_{\text{ion}}^*}{10^{49} \text{ s}^{-1}} \right)^{-1/3} \left(\frac{n_H}{1000 \text{ cm}^{-3}} \right)^{-4/3} \quad (36)$$

when $\nu \lesssim \nu_S$. For star-formation rates of $10 \text{ M}_\odot \text{ yr}^{-1}$, similar to those found in M82, we can already see that there will typically be several hundred parsecs of synchrotron emitting material on any line of sight before hitting an H II region. Since the typical line of sight through M82 has length $\sim R_{\text{SB}} \approx 250 \text{ pc}$, there is about one Strömgren sphere on any line of sight, if most of the massive stars are isolated.

In Figure 2, I show the effective absorption coefficient from Strömgren spheres around O stars for densities $1 - 10^6 \text{ cm}^{-3}$. The absorption coefficients reach a plateau at low frequency, with a value that depends on hydrogen density. At high frequencies, the absorption coefficients for different hydrogen densities all have the same value. In this case, the cross section of Strömgren spheres with volume V_S is $V_{S\text{AHH}}$ (section 2.1.1), which does not depend on density.

3.2 H II regions around Super Star Clusters: A simple model

Much of the star-formation in starburst galaxies occurs in bound super star clusters (SSCs; e.g., O’Connell et al. 1995; Melo et al. 2005; Smith et al. 2006). The SSCs have a mass function that can be described with a Schechter mass function

$$\frac{dN}{dM_*} = C M_*^{-2} \exp\left(-\frac{M_*}{M_c}\right), \quad (37)$$

where M_c is a cutoff mass around $5 \times 10^6 \text{ M}_\odot$ in starbursts (Meurer et al. 1995; McCrady & Graham 2007), and the mass function applies only above a lower mass limit M_l , which I take to be 1000 M_\odot .

Now suppose that

- The initial mass function of SSCs has the same form as the observed mass function.
- The ionizing photon luminosity Q_{ion} of a SSC is directly proportional to its stellar mass. Furthermore, Q_{ion} is assumed to be a reverse step function: a constant for SSCs of an age less than $t_{\text{ion}} = 10 \text{ Myr}$, and then zero afterwards.
- The starburst has been continuously forming stars (and SSCs) at a constant rate for a time $t_{\text{burst}} > t_{\text{ion}}$.

Then I can construct a mass function of SSCs with ionizing stars:

$$\frac{dN_{\text{ion}}}{dM_*} = C_{\text{ion}} M_*^{-2} \exp(-M_*/M_c), \quad (38)$$

which is normalized so that $M_*^{\text{ion}} = \text{SFR} \times t_{\text{ion}} = \int_{M_l}^{\infty} C_{\text{ion}} M_*^{-1} \exp(-M_*/M_c) dM_*$. For $M_l = 1000 \text{ M}_\odot$ and $M_c = 5 \times 10^6 \text{ M}_\odot$,

$$C_{\text{ion}} = 0.126 \text{ SFR } t_{\text{ion}}. \quad (39)$$

Under my assumptions, these ionizing photons all come from stars with ages less than t_{ion} . We can therefore convert the star-formation into the mass of the SSCs containing ionizing stars as $\text{SFR} = M_*^{\text{ion}}/t_{\text{ion}}$:

$$Q_{\text{ion}} = 2.18 \times 10^{46} \text{ ph s}^{-1} \left(\frac{M_*^{\text{ion}}}{\text{M}_\odot} \right). \quad (40)$$

Plugging in typical values for an SSC in a starburst, I find

$$R_S = 8.8 \text{ pc} \left(\frac{M_*}{10^6 \text{ M}_\odot} \right)^{1/3} \left(\frac{n_H}{1000 \text{ cm}^{-3}} \right)^{-2/3}. \quad (41)$$

The absorption coefficient at low ν from H II regions is, after integrating the SSC mass function from M_l to infinity,

$$\alpha_{\text{eff}} = \frac{3C_{\text{ion}}\pi R_0^2}{V M_0^{2/3}} \left[\frac{\exp(-M_l/M_c)}{M_l^{1/3}} - \frac{\Gamma(2/3, M_l/M_c)}{M_c^{1/3}} \right], \quad (42)$$

where I take $R_S = R_0(M/M_0)^{1/3}$. For the case when $M_l = 1000 \text{ M}_\odot$ and $M_c = 5 \times 10^6 \text{ M}_\odot$, I find

$$\alpha_{\text{eff}} = (4600 \text{ pc})^{-1} \left(\frac{\text{SFR}}{\text{M}_\odot \text{ yr}^{-1}} \right) \left(\frac{t_{\text{ion}}}{10 \text{ Myr}} \right) \times \left(\frac{n_H}{1000 \text{ cm}^{-3}} \right)^{-4/3} \left(\frac{R_{\text{SB}}}{250 \text{ pc}} \right)^{-2} \left(\frac{h_{\text{SB}}}{100 \text{ pc}} \right)^{-1} \quad (43)$$

The absorption coefficient is smaller than in the case of each O star having its own Strömgren sphere. This can be seen if we assume each cluster has N_* O stars, each with the same ionizing luminosity. Since the Strömgren radius goes only as $N_*^{1/3}$, the cross section of each H II region increases only as $N_*^{2/3}$. The number of Strömgren spheres instead decreases as N_*^{-1} , meaning the effective absorption coefficient is proportional to $N_*^{-1/3}$: clustered stars are not as effective at obscuration. Essentially, clustering preserves the filling factor that is ionized, but since the regions that are ionized are spatially correlated – the ionized regions at the front

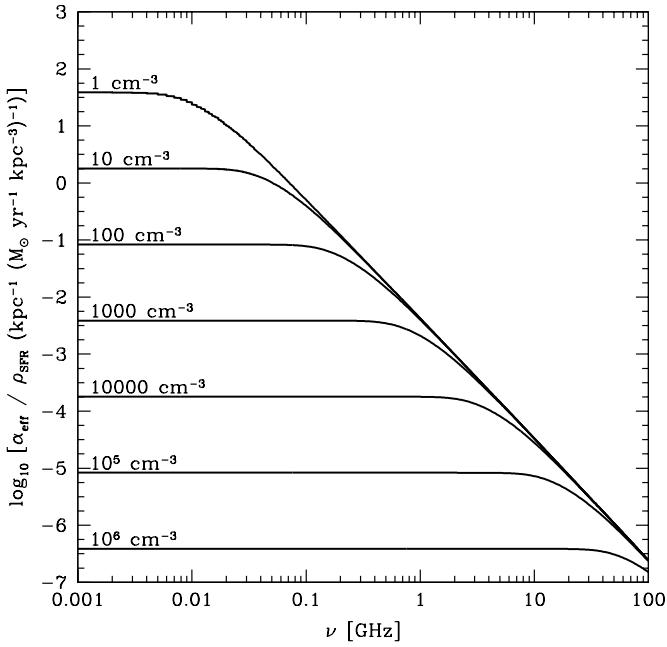


Figure 3. Effective absorption coefficient for H II regions of various densities, as normalized to a volumetric star-formation rate of $1 \text{ M}_\odot \text{ yr}^{-1} \text{ kpc}^{-3}$. This plot shows the case when O stars are all within ‘simple’ SSCs surrounded by H II regions, in which the ionizing photon luminosity of a SSC remains constant for $t_{\text{ion}} = 10 \text{ Myr}$ and then shuts off. The low mass cut-off is $M_l = 1000 \text{ M}_\odot$, and the characteristic highest mass is $M_c = 5 \times 10^6 \text{ M}_\odot$.

of a large H II region already obscures the ionized volume behind it – the covering factor is decreased.

I plot in Figure 3 the effective absorption coefficients for Strömgren spheres around SSCs with masses above 1000 M_\odot and a cutoff of $5 \times 10^6 \text{ M}_\odot$. The α_{eff} are indeed lower than in the case of isolated O stars, but the functional form is basically the same, with a plateau at low frequencies that depends on hydrogen density and an asymptotic form at high frequencies that is independent of hydrogen frequency.

3.3 H II regions around Super Star Clusters: A model that includes aging

My assumption in the previous subsection – that SSCs behave like light bulbs, emitting ionizing photons for some time before shutting off – is simplistic. In fact, with models such as Starburst99, it is possible to predict how the ionizing photon generation rate evolves for stellar populations of various ages (Leitherer et al. 1999). In principle, one can then use a known star-formation history to accurately predict the cluster mass and age distribution function, and then integrate the cross sections to get an effective absorption coefficient.

As an example, I will consider the case when the star-formation rate has been constant for a duration t_{burst} , before which it was zero. The SSC distribution function is then assumed to have the form

$$\frac{dN}{dM_\star dt} = \frac{C_{\text{aging}}}{t_{\text{burst}}} M_\star^{-2} \exp\left(-\frac{M_\star}{M_c}\right) \quad (44)$$

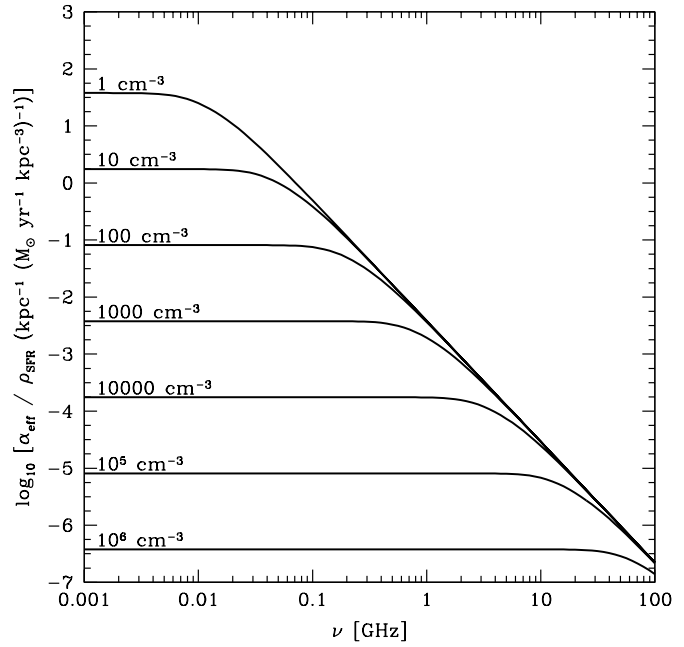


Figure 4. Effective absorption coefficient for H II regions around aging SSCs of various densities, as normalized to a volumetric star-formation rate of $1 \text{ M}_\odot \text{ yr}^{-1} \text{ kpc}^{-3}$. The starburst age is assumed to be 10 Myr . The low mass cutoff is $M_l = 1000 \text{ M}_\odot$, and the characteristic highest mass is $M_c = 5 \times 10^6 \text{ M}_\odot$.

where M_\star is the mass of stars initially formed in the cluster, and t is the age of the cluster. The SSC initial mass function then has the same form as before, in equation 37. The normalization C_{aging} is again set by integrating over masses to get the star-formation rate, $\text{SFR} = \int_{M_l}^{\infty} M_\star dN/(dM_\star dt) dM_\star$. For my standard values of $M_l = 1000 \text{ M}_\odot$ and $M_c = 5 \times 10^6 \text{ M}_\odot$, I find $C_{\text{aging}} = 0.126 \text{ SFR } t_{\text{burst}}$.

I find the effective absorption coefficient by integrating the H II region absorption cross section over different cluster masses and ages:

$$\alpha_{\text{eff}} = \int_{M_l}^{\infty} \int_0^{t_{\text{burst}}} \frac{dN}{dM_\star dt} \frac{1}{V} \sigma(Q_{\text{ion}}(M_\star, t), \nu) dt dM_\star. \quad (45)$$

The starburst volume is here denoted as V . The ionizing photon rate Q_{ion} for a stellar population of age t is given in Leitherer et al. (1999).

I show the resulting α_{eff} for a 10 Myr old continuously forming starburst in Figure 4. The results are very similar to the simply-modelled SSCs (as plotted in Figure 3).

4 FITS TO M82’S RADIO SPECTRUM

The brightest starburst in the radio sky is M82. Located $\sim 3.6 \text{ Mpc}$ away (as adopted in this section from Freedman et al. 1994, although Sakai & Madore 1999 measure a distance of 3.9 Mpc), it has a total infrared luminosity of $5.9 \times 10^{10} L_\odot$ (Sanders et al. 2003), corresponding to a Salpeter IMF star-formation rate of $10 \text{ M}_\odot \text{ yr}^{-1}$ (Kennicutt 1998). Most of the radio and infrared emission

comes from a region of radius ~ 250 pc (Goetz et al. 1990; Williams & Bower 2010). The starburst is viewed essentially edge-on from Earth.

Williams & Bower (2010) obtained high quality radio observations in the GHz range using the Allen Telescope Array (ATA). They also compile interferometric and single-dish observations in the frequency range of 20 - 100 GHz, which are useful in constraining free-free emission. Noting a systematic offset in the single-dish observations, Williams & Bower (2010) do not include single-dish observations in their modelling, a practice I follow for observations above 1 GHz. Unlike the other bright starburst, NGC 253 (Carilli 1996), most of the radio emission comes from the starburst itself rather than the host galaxy (Basu et al. 2012). This is especially important at low frequencies, where galaxies are frequently unresolved: the starburst may be obscured by its own H II regions, but the host galaxy is likely to be unobscured.

Besides these observations, there are quite a few observations below 1 GHz, although the errors are naturally larger (see Table 1). In theory, the wide frequency coverage of the data, spanning from 22.5 MHz to 92 GHz, makes M82 a good choice for spectral modelling. However, I note that many different instruments were used in collecting this data, with widely disparate beam sizes. For most of the measurements below 1 GHz, not even the host galaxy (diameter $\sim 10'$) is resolved. In contrast, the ATA has a synthesized beam diameter of 4.2 at 1 GHz and $35''$ at 7 GHz, sufficient to resolve the host galaxy (Williams & Bower 2010). The VLA and GMRT low frequency observations also had beam sizes small enough to resolve the host galaxy (and the starburst itself for the GMRT; Cohen et al. 2007; Basu et al. 2012). The radio flux at 333 MHz from the GMRT is between those of the unresolved 178 and 750 MHz measurements, suggesting that little flux is missing. The radio flux from the 74 MHz VLA sky survey is only $\sim 2/3$ of that from the unresolved 57.5 and 86 MHz measurements, which may mean that some flux is missing (perhaps from the host galaxy). However, the error bars are very large, so it is unclear this is the case; furthermore, the 74 MHz VLA sky survey did report integrated fluxes even for resolved sources (Cohen et al. 2007). In any case, the 74 MHz VLA sky survey reports a major axis size for M82 of $66''.9 \pm 2''.8$ (smaller than the beam size), indicating that the majority of M82's 74 MHz radio emission comes from within 600 pc of its centre (Cohen et al. 2007). Thus, it appears the starburst itself is emitting at these frequencies, not just the host galaxy.

For this paper, I largely ignore the different beam sizes and assume all of the radio data points accurately measure the radio flux from the inner starbursting region of M82. The results should therefore be treated cautiously, until this assumption can be verified by high resolution studies at low frequency, such as with the GMRT or the Jansky VLA. My primary purpose here is to demonstrate how low frequency radio spectra can be fit with the new free-free absorption models, and to show what kinds of information can be extracted.

4.1 Procedure

I fit the properties of the H II regions. The star-formation rate sets the number of H II regions and is

allowed to be $\text{SFR} = 0.625, 1.25, 2.5, 5, 10, 20 \text{ M}_\odot \text{ yr}^{-1}$. The electron density is allowed to be $n_e = 100, 200, 300, 600, 1200, 1800 \text{ cm}^{-3}$, and the electron temperature can be $T_e = 5000, 7500, 10000, 12500, 15000, 20000 \text{ K}$; these set the Strömgren radius and turnover frequency for each H II region. Finally, I set the scale height of the starburst h_{SB} , which affects the covering fraction, to be 100 pc. I consider both a scenario where the H II regions surround individual O stars and where the H II regions surround SSCs with a low mass cutoff at 1000 M_\odot and a high mass cutoff at $5 \times 10^6 \text{ M}_\odot$; the SSCs are modeled either as simple or aging continuously. In the aging SSC model, I assume M82's starburst is 15 Myr old (Förster Schreiber et al. 2003).

I then suppose the radio emission to be a combination of synchrotron and free-free emission. Rather than running models of cosmic ray e^\pm populations, a process which would introduce many free parameters, I use the phenomenological function form of Williams & Bower (2010) for the unab- sorbed synchrotron spectrum:

$$\log_{10} \left(\frac{S_{\text{nt}}^{\text{unabs}}}{\text{Jy}} \right) = \mathcal{A} + \mathcal{B} \log_{10} \left(\frac{\nu}{\text{GHz}} \right) + \mathcal{C} \left[\log_{10} \left(\frac{\nu}{\text{GHz}} \right) \right]^2 \quad (46)$$

In this formula, $-\mathcal{B}$ corresponds to the spectral index, thought to be near $0.6 - 0.8$, and \mathcal{C} is the spectral curvature, thought to be ≤ 0 due to increasing synchrotron and Inverse Compton losses for electrons and high energies (Thompson et al. 2006).

Any H II regions that contribute to free-free absorption must also emit free-free emission. The ionizing photon luminosity that supports these H II regions, as parametrized by the star-formation rate, is directly related to their thermal emission as

$$S_{\text{min-ff}}^{\text{unabs}} = \mathcal{D}_{\text{min}} \left(\frac{\nu}{\text{GHz}} \right)^{-0.1} \quad (47)$$

$$\mathcal{D}_{\text{min}} = 0.22 \text{ Jy} \left(\frac{\text{SFR}}{\text{M}_\odot \text{ yr}^{-1}} \right) \left(\frac{T_e}{10^4 \text{ K}} \right)^{0.45} \left(\frac{D}{3.6 \text{ Mpc}} \right)^{-2} \quad (48)$$

using the Q_{ion} from equation 30 (Condon 1992). However, it is possible that there is ionized gas which does contribute to the free-free emission but not to absorption. This can happen if there is a population of small but dense H II regions with low covering fraction, such as ultracompact H II regions. I therefore fit an additional component of free-free emission:

$$S_{\text{add-ff}}^{\text{unabs}} = \mathcal{D}_{\text{add}} \left(\frac{\nu}{\text{GHz}} \right)^{-0.1} \text{ Jy}. \quad (49)$$

The total predicted radio spectrum of M82 is then

$$S_\nu^{\text{pred}} = [S_{\text{nt}}^{\text{unabs}} + S_{\text{min-ff}}^{\text{unabs}} + S_{\text{add-ff}}^{\text{unabs}}] \frac{F}{F_{\text{unabs}}}; \quad (50)$$

I use the edge-on disc value of F/F_{unabs} as given in equation 23.

For each combination of parameters describing radio absorption ($\text{SFR}, n_e, T_e, h_{\text{SB}}$), I use χ^2 fitting to find the values of $\mathcal{A}, \mathcal{B}, \mathcal{C}$, and \mathcal{D}_{add} that best fit the radio spectrum. The values of \mathcal{A} are allowed to range from 0 to 2, with a spacing of 0.01; I try values of \mathcal{B} from -0.9 to -0.3, with a spacing of 0.02; \mathcal{C} ranges from -0.2 to 0.1, with a spacing of 0.02; and \mathcal{D}_{add} ranges from 0 to 1 with a spacing of 0.025. Then, I compare the χ^2 values for the fits for each absorption parameter set to find the best-fitting model.

Table 1. Low Frequency Radio Data for M82

ν (MHz)	S_ν (Jy)	Reference	Synthesized beam size (θ) ^a	Instrument
22.5	39 ± 5	Roger, Costain, & Stewart (1986)	$66' \times 102'$	Dipole array, Dominion Radio Astrophysical Observatory
38	23 ± 3	Kellermann, Pauliny-Toth, & Williams (1969) ^b	$45' \times 45' \sec \zeta$	Aperture-synthesis system, Mullard Radio Astronomy Observatory
57.5	29 ± 6	Israel & Mahoney (1990)	$7'0 \times 6'5$	Aperture-synthesis system, Clark Lake Radio Observatory
74	18.36 ± 1.86	Cohen et al. (2007)	$80''$	VLA
86	27.8 ± 3.8	Artyukh et al. (1969); Laing & Peacock (1980)	$\sim 12' \times 12'$	DKR-1000
151	$16.82^c \pm 0.62$	Baldwin et al. (1985); Hales et al. (1991)	$4'2 \times 4'2 \cos \delta$	6C aperture-synthesis telescope
178	15.3 ± 0.7	Kellermann et al. (1969) ^b	$23' \times 18' \sec \zeta$	Aperture-synthesis system, Mullard Radio Astronomy Observatory
333	14 ± 1	Basu et al. (2012)	$22'' \times 15''$	GMRT
750	10.7 ± 0.5	Kellermann et al. (1969) ^b	$18'5 \times 18'5$	Green Bank Telescope

^a: The zenith angle is ζ and the declination is δ .

^b: As recalibrated by Klein et al. (1988).

^c: Average of two measurements.

As a counterpoint to these models, I also considered models where there was no free-free absorption, and uniform slab models. In each case, \mathcal{A} , \mathcal{B} , and \mathcal{C} were free parameters. For the no-absorption models, I simply added a free-free emission component parametrized by \mathcal{D}_{add} . In the uniform slab models, the electron temperature T_e was a free parameter, with the same values as in the discrete H II region models. I then chose \mathcal{D} to fit the free-free emission and absorption, where the absorption coefficient is directly related to the emission as $\alpha_\nu = j_\nu / B_\nu(T_e) = S_\nu D^2 / (2\pi B_\nu(T_e) R_{\text{SB}}^2 h)$, using the blackbody source function $B_\nu(T_e)$. In each case, I used χ^2 fitting to the radio data to select the best-fitting parameters. While I fit to all of the radio data for the no-absorption models, for the uniform slab case I only used data points above 1 GHz. When I include the low frequency data, the best-fitting models invariably have no free-free absorption or emission.

I also redid the fits using only the radio data points where the beam size was less than $10'$, to see how measurements with large beam sizes were affecting my results.

4.2 Results

The best-fitting results with discrete H II regions, whether surrounding individual O stars or SSCs, are better at reproducing the low frequency radio spectrum of M82 than either a fit without absorption or a uniform slab model (Table 2). The best-fitting individual O star model is shown in Figure 5, the best-fitting simple SSC model is shown in Figure 6, and the best-fitting aging SSC model is shown in Figure 7. While the simple and aging SSC models both have low temperatures and densities, the best-fitting individual O star model has higher density and temperature. However, there are several conclusions that are similar in each of the three cases:

- The unabsorbed synchrotron spectrum is fairly flat, with an intrinsic nonthermal spectral index of ~ 0.6 , which

is lower than the typical values of $\sim 0.8 - 0.9$ for normal spiral galaxies (e.g., Niklas et al. 1997). Previously, this has been attributed to free-free absorption, but my models show this is not necessarily the case: the spectrum really could be intrinsically flat. My values are basically consistent with the fit of Williams & Bower (2010), $\mathcal{B} = -0.56 \pm 0.02$.

- The unabsorbed synchrotron spectrum is curved, becoming steeper at higher frequency. The derived intrinsic nonthermal spectral curvature in the best-fitting models is consistently $\mathcal{C} \approx -0.08$. Curvature is expected if ionization and bremsstrahlung losses are responsible for flattening the spectrum (Hummel 1991; Thompson et al. 2006). This curvature is slightly less than that of Williams & Bower (2010), $\mathcal{C} = -0.12 \pm 0.03$.

- The covering fraction of the H II regions is of order $\sim 1/2$, and the filling fraction ranges from 0.2 to 3%. As a result, most of the radio flux is transmitted even at low frequencies, with transmission fractions of $\sim 60 - 75\%$. At 1 GHz, free-free absorption reduces the observed flux by only a few percent.

- These models require low ionizing photon luminosities relative to M82's star-formation rate of $10 M_\odot \text{ yr}^{-1}$. Partly, this is because the low frequency radio spectrum is consistent with only small amounts of free-free absorption. The ionizing photon luminosity powering the absorbing H II regions is equivalent to a star-formation rate of only $\lesssim 1 M_\odot \text{ yr}^{-1}$. Even when I include an additional non-absorbing free-free emission component, the equivalent star-formation rate is only $\sim 2 M_\odot \text{ yr}^{-1}$. The thermal fraction at 1 GHz in these models is only $\sim 5\%$.

In contrast to the discrete H II region models, the best-fitting model with no free-free absorption (solid grey line in Figures 5 - 7) requires strong intrinsic spectral curvature ($\mathcal{C} = -0.18$) and a flatter synchrotron spectrum ($\mathcal{B} = -0.52$) in order to not overproduce the observed low frequency emission. However, at the lowest frequencies, the spectral curvature then suppresses the radio emission too much, leading to

Table 2. M82 Radio Spectrum Fits

Quantity Data	No Absorption All ^a	Uniform Slab ≥ GHz	Individual O Stars All ^a	Simple SSCs		Aging SSCs	
				All	$\theta < 10'$ ^b	All	$\theta < 10'$ ^b
$\text{SFR}_{\text{abs}} (\text{M}_{\odot} \text{ yr}^{-1})^c$	0.625	0.625	0.625	1.25	1.25
$n_e (\text{cm}^{-3})$...	35	600	100	300	100	300
$T_e (\text{K})$...	20000	20000	7500	20000	7500	20000
$h (\text{pc})$	100	100	100	100	100	100	100
\mathcal{A}	0.91	0.95	0.93	0.94	0.92	0.94	0.92
\mathcal{B}	-0.52	-0.60	-0.58	-0.60	-0.56	-0.58	-0.56
\mathcal{C}	-0.18	-0.06	-0.10	-0.08	-0.14	-0.08	-0.14
$\mathcal{D}_{\text{min}}^d$	0.19	0.12	0.19	0.23	0.36
$\mathcal{D}_{\text{add}}^e$	0.65	0.30	0.33	0.35	0.45	0.13	0.28
χ^2	96.0 (75.5 ^a)	69.7 (657 ^j)	83.0 (75.8 ^a)	81.8	74.6	81.6	74.1
f_{cover}	...	100%	43%	50%	25%	57%	29%
f_{fill}	...	100%	0.23%	2.3%	0.57%	2.8%	0.70%
$f_{\text{therm}} (1 \text{ GHz})^f$	7.4%	3.4%	6.1%	5.4%	7.2%	4.1%	7.1%
$F/F_{\text{unabs}}(\nu \rightarrow 0)^g$...	0%	74.6%	61.9%	81.7%	64.8%	83.4%
$F/F_{\text{unabs}}(1 \text{ GHz})^h$...	96.7%	97.8%	96.5%	97.9%	97.3%	98.4%
$P_{\text{HII}}/k (\text{K cm}^{-3})^i$...	6.9×10^5	3.6×10^7	2.3×10^6	1.8×10^7	2.3×10^6	1.8×10^7
$\text{SFR}_{\text{em}} (\text{M}_{\odot} \text{ yr}^{-1})$	2.9	0.99	1.7	2.4	2.1	1.8	2.1

^a: The best-fitting parameters for these models are the same whether all data are included or just those with beam sizes less than 10 arcminutes. The χ^2 value when only data with beam sizes less than 10 arcminutes is given in parentheses.

^b: Fluxes for observations with beam sizes less than 10 arcminutes (see Table 1).

^c: Effective star-formation rate, which sets the ionizing photon luminosity of the starburst. This sets both the number of H II regions and the amount of free-free emission.

^d: Thermal free-free emission at 1 GHz from the H II regions responsible for free-free absorption. This sets a floor on the amount of free-free emission.

^e: Additional free-free emission from ionized gas that does not contribute to free-free absorption in my model (e.g., from more compact, denser H II regions). This is a free parameter.

^f: Fraction of the flux at 1 GHz which is thermal free-free emission.

^g: Fraction of the radio flux transmitted by the free-free absorbing H II regions at extremely low frequencies. The effects of free-free absorption in other phases or synchrotron self-absorption are not included.

^h: Fraction of the radio flux transmitted by the free-free absorbing H II regions at 1 GHz.

ⁱ: Derived thermal pressure in H II regions, $3n_e T_e$.

^j: In selecting the uniform slab model, χ^2 was minimized for data above 1 GHz; this value is 69.7. However, if all radio data is included, the total χ^2 increases to 657.

a relatively poor fit. The radio flux in the uniform slab model (long-dashed line) plummets rapidly and cannot explain the data points below ~ 300 MHz at all.

The effects of free-free absorption on the spectrum shape are concentrated within a finite frequency band. At high frequencies, the H II regions are transparent. At low frequencies, the H II regions are completely opaque, and α_{eff} reaches some constant value; this changes the normalization of the spectrum, but not its intrinsic shape. These effects can be described more quantitatively in terms of the total spectral index $\tilde{\mathcal{B}}$ and spectral curvature $\tilde{\mathcal{C}}$:

$$\tilde{\mathcal{B}} \equiv \frac{d \log_{10} S_{\nu}^{\text{pred}}}{d \log_{10} \nu} \quad (51)$$

$$\tilde{\mathcal{C}} \equiv \frac{d^2 \log_{10} S_{\nu}^{\text{pred}}}{d(\log_{10} \nu)^2}; \quad (52)$$

these quantities differ from \mathcal{B} and \mathcal{C} in that they include free-free emission and absorption. I show how $\tilde{\mathcal{B}}$ and $\tilde{\mathcal{C}}$ vary with frequency in Figure 8 for the best-fitting models⁵. Free-free absorption (the difference between black and grey lines) flattens the spectrum (higher $\tilde{\mathcal{B}}$) between ~ 0.1 –1 GHz: this

is the regime where H II regions become optically thick. The resulting pulse in $\tilde{\mathcal{B}}$ is narrower when H II regions surround individual O stars (dotted lines) instead of SSCs: in that model, the H II regions all have the same size, with the same turnover frequency, instead of the range of turnover frequencies for SSCs. A pulse also appears in the spectral curvature in this frequency range. One potential issue for studies looking for intrinsic nonthermal curvature in the radio spectrum is that either free-free absorption or emission affect most observable radio frequencies. Only at frequencies of a few GHz or, paradoxically, below ~ 30 MHz where α_{eff} is constant, does the intrinsic curvature dominate over that introduced by free-free absorption or emission.

One motivation for studying free-free absorption is to calculate the thermal pressure in H II regions from the density and temperature (c.f., Carilli 1996). Even in my best-fitting models, the pressure varies by an order of magnitude. It is extremely high in the individual O star model, with $P/k = 4 \times 10^7 \text{ K cm}^{-3}$. In my SSC models, it is only $P/k = 2 \times 10^6 \text{ K cm}^{-3}$. Numerous studies have inferred the pressure of M82's H II regions, using infrared and optical spectroscopy. Smith et al. (2006) found a fairly high pressure of $P/k = (1-2) \times 10^7 \text{ K cm}^{-3}$ for the H II region around the M82 A-1 super star cluster, still less than the individual star model, but much greater than in the SSC models.

⁵ Note the use of base 10 logarithms. While $\tilde{\mathcal{B}} = d \ln S_{\nu}^{\text{pred}} / d \ln \nu$, $\tilde{\mathcal{C}} = \ln 10 \times d^2 \ln S_{\nu}^{\text{pred}} / d(\ln \nu)^2$

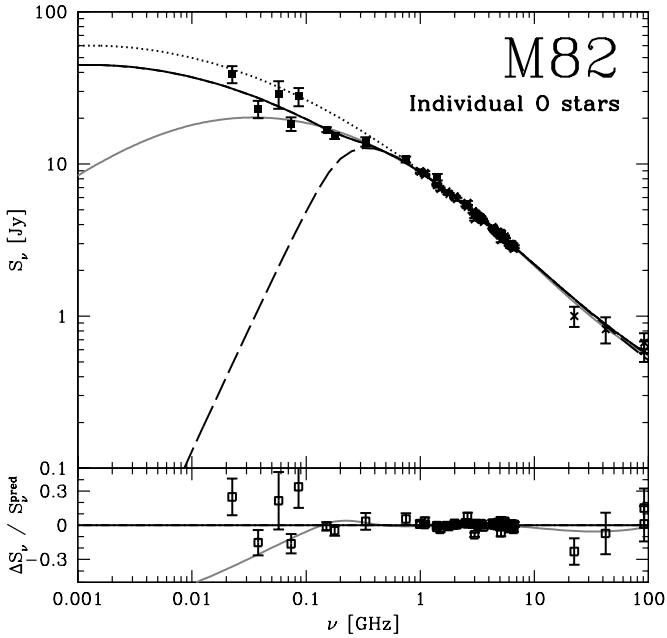


Figure 5. The effects of free-free absorption on M82’s radio spectrum, for H II regions surrounding individual O stars. The solid black line is the best-fitting to the free-free absorption, and the dotted line is what that fit spectrum would be without absorption. The grey solid line is the best possible fit with no absorption, though it does include free-free emission. I show a uniform slab fit to the ≥ 1 GHz radio spectrum as the dashed line. The residuals are plotted on the bottom.

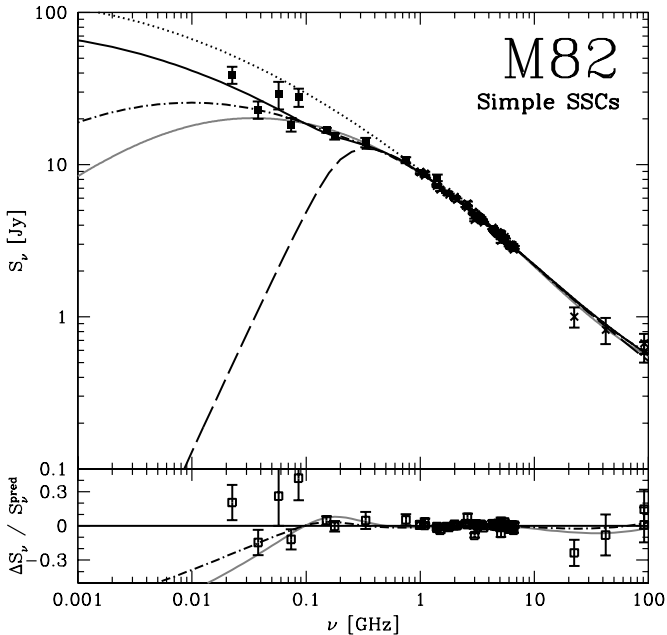


Figure 6. A model of the free-free absorption on M82’s radio spectrum, using the simple super star cluster assumptions described in section 3.2. I plot the best-fitting model to the radio data with beam sizes $< 10''$ as the dash-dotted line. The other line styles are the same as in Figure 5.

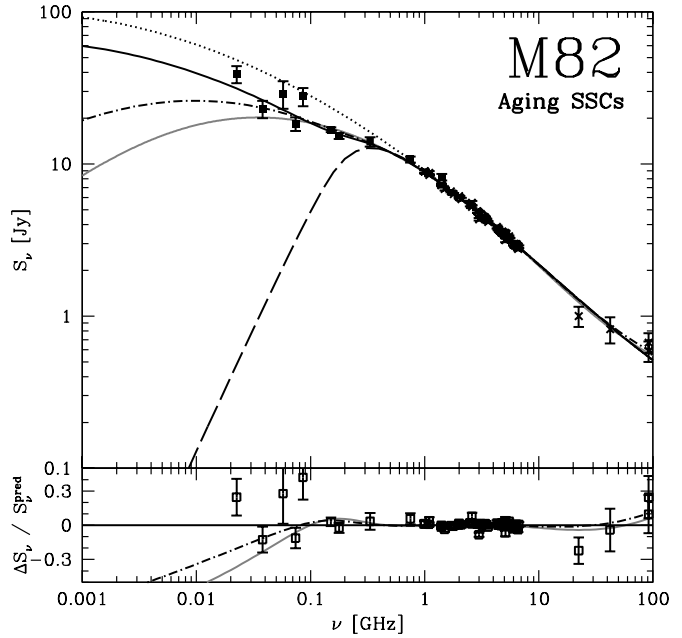


Figure 7. A model of the free-free absorption on M82’s radio spectrum, where the model now accounts for how the ionizing photon luminosity of SSCs evolve as they age. I plot the best-fitting model to the radio data with beam sizes $< 10''$ as the dash-dotted line. The other line styles are the same as in Figure 5.

Note that M82 A-1 is relatively large ($\sim 10^6 M_{\odot}$) compared to the small SSCs that would be expected to dominate the free-free absorption. Westmoquette et al. (2007) found lower pressures of $P/k = (5 - 10) \times 10^6 \text{ K cm}^{-3}$ in most M82 H II regions, though these pressures are still several times larger than what I find in my SSC models. Lord et al. (1996) inferred H II region pressures of $P/k = 3 \times 10^6 \text{ K cm}^{-3}$, based on infrared diagnostics of the surrounding denser and colder photodissociation regions. In any case, though, because of the range of densities I allowed for discrete H II regions, the pressures are necessarily higher than what I would find with a uniform slab model ($\sim 7 \times 10^5 \text{ K cm}^{-3}$; compare with the similar results for NGC 253 in Carilli 1996).

The low ionizing photon luminosities I derive are worrying, especially since I allow for ‘hidden’ free-free emission from compact H II regions that do not contribute to absorption. The low luminosities may be because of the large errors and sparseness of the high frequency data. On the other hand, thermal dust emission probably contributes to the highest frequency data points at some level, and there may be spinning dust emission as well, but including any dust emission would just tighten the constraints on the free-free emission. It is possible, though, that the amount of free-free emission really is low in starburst galaxies – perhaps not a surprising hypothesis given that starbursts are dusty places (c.f., Petrosian, Silk, & Field 1972). Or perhaps some ultraviolet photons escape into the hot superwind phase that likely fills much of the starburst volume, instead of ionizing the molecular gas. If so, then free-free emission is not necessarily a simple star-formation rate indicator in starbursts: its strength depends somehow on the radiative transfer in dusty

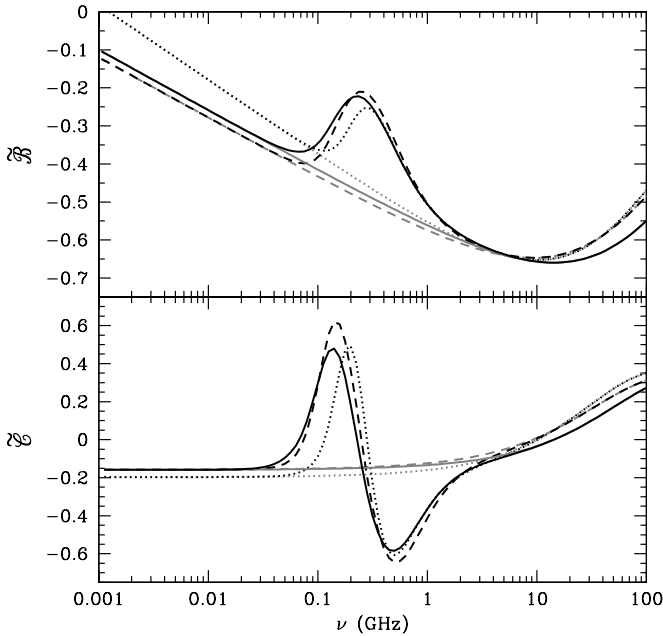


Figure 8. How free-free absorption affects the total spectral index $\tilde{\beta}$ (top) and total spectral curvature \tilde{C} (bottom). I show these values with (black) and without (grey) free-free absorption. The line styles are for different M82 models; dotted is individual O stars, dashed is simple SSCs, and solid is aging SSCs. Free-free absorption introduces a pulse in the spectral index and curvature, as H II regions transition from being transparent to opaque with decreasing frequency.

environments, and it is buried even more than expected by synchrotron emission.

As I noted before, though, these results must be considered preliminary, since the low frequency data so vital in constraining free-free absorption comes from many instruments with different beam sizes. A future low frequency survey of M82 that resolves the starburst would ensure that flux from the surrounding galaxy is not making M82’s starburst appear brighter than it really is; such a survey can be done with the GMRT, VLA, or LOFAR.

When I fit only the data with beam sizes smaller than $10'$, the basic conclusion that most of the flux is transmitted stands. The best-fit individual O stars model is actually unchanged with these data. However, the models of Strömgren spheres around SSCs now fit better for somewhat higher densities (300 cm^{-3}) and much higher temperatures (20000 K). The best-fitting spectral index is now 0.56, with a curvature $C = -0.14$, higher than before. These models have even lower H II region covering fractions (25 – 30%), but comparable thermal fractions (5 – 7%). Therefore, the environments of the H II regions are not too well constrained, and better radio data is needed, but absorption from discrete H II regions are adequate so far to explain the radio spectrum.

Besides better low frequency data, it would be helpful to have high quality observations at 10 - 100 GHz. Then it may be possible to meaningfully detect the flattening from free-free emission, if it is present. The Jansky VLA is able to observe at up to 50 GHz (Perley et al. 2011), and with

its high sensitivity, the shape of the spectrum can be more meaningfully constrained. Moreover, as a single instrument, there would be fewer worries about systematics when comparing between data at different frequencies. Furthermore, it has high spatial resolution, so it can actually measure the characteristic sizes of H II regions, in particular searching for small, high density H II regions. Another possibility is to use radio recombination lines, also observable with the Jansky VLA (Kepley et al. 2011), which constrain not only the ionizing photon luminosity of a starburst, but which density and temperatures the ionized gas has. I note that Rodriguez-Rico et al. (2004) found using H53 α and H92 α radio recombination lines an ionizing photon luminosity of $1.6 \times 10^{53} \text{ s}^{-1}$ for M82, equivalent to a star-formation rate of $0.7 \text{ M}_{\odot} \text{ yr}^{-1}$, compatible with the low ionizing photons I find here. On the other hand, Puxley et al. (1989) deduced an ionizing luminosity of $1.1 \times 10^{54} \text{ s}^{-1}$ also using the H53 α line, which would correspond to a star-formation rate of $5 \text{ M}_{\odot} \text{ yr}^{-1}$. This is significantly greater than what I find with my fits, but still a factor of ~ 2 lower than the infrared-derived star-formation rate. Future radio recombination line studies may clarify the situation.

5 WHERE DO THE RADIO SPECTRA OF STARBURSTS REALLY END?

The premise of this work is that free-free absorption from H II regions only partially covers starburst galaxies, and starbursts still emit quite a lot of radio emission at low frequencies. However, the starburst radio spectrum cannot continue indefinitely to zero frequency. The presence of more diffuse volume-filling phases of ionized gas within starbursts will provide free-free absorption. In addition, the purely nonthermal process of synchrotron self-absorption eventually must cut off the radio spectrum of starburst galaxies even if there is no diffuse ionized gas. In this section, I calculate the effects of these additional processes to find when starbursts should have true cutoffs in their radio spectra.

5.1 Free-free absorption in starburst winds

The high rate of supernovae in starburst galaxies occurring within a relatively small space is expected to excavate a hot phase of the ISM (McKee & Ostriker 1977; Heckman, Armus, & Miley 1990). The hot ISM erupts as a starburst-wide superwind, and is low density, but high in pressure, temperature, and, it is thought, filling factor (e.g., Chevalier & Clegg 1985). Gas emitting in soft X-rays is indeed observed in many starbursts, though Strickland & Stevens (2000) argues that this emission comes from a cooler phase with lower filling factor than the actual wind. In addition, *Chandra* detected diffuse 6.7 keV iron line emission in M82 that supports the presence of 10^8 K gas (Strickland & Heckman 2007).

Strickland & Heckman (2009) give the central density of the superwind as

$$\rho_c = 0.930 \frac{\beta^{3/2}}{\epsilon_{\text{therm}}^{1/2}} \frac{\dot{M}^{3/2}}{\dot{E}^{1/2} (\pi R^2)} \quad (53)$$

and the central temperature for a completely ionized wind as

$$T_c = \frac{0.8 m_H \epsilon_{\text{therm}} \dot{E}}{k \beta \dot{M}}. \quad (54)$$

In these equations, $\epsilon_{\text{therm}} \approx 0.5$ is the fraction of supernova energy that ends up in thermal energy of the plasma, $\beta \approx 2$ is the mass-loading fraction⁶ (Strickland & Heckman 2009). They give the mass injection rate from supernovae and stellar winds as

$$\dot{M} = 0.14 \text{ M}_\odot \text{ yr}^{-1} \left(\frac{\text{SFR}}{\text{M}_\odot \text{ yr}^{-1}} \right) \quad (55)$$

and the energy injection rate from supernovae as

$$\dot{E} = 2.9 \times 10^{41} \text{ erg s}^{-1} \left(\frac{\text{SFR}}{\text{M}_\odot \text{ yr}^{-1}} \right) \quad (56)$$

where I have converted between SFR above 1 M_\odot and the SFR for a Salpeter IMF from 0.1 to 100 M_\odot using $\text{SFR}(\geq 1 \text{ M}_\odot) = 0.45 \text{ SFR}$. Then, in numerical terms, I have

$$n_c = 0.011 \text{ cm}^{-3} \left(\frac{\beta}{2} \right)^{3/2} \left(\frac{\epsilon_{\text{therm}}}{0.5} \right)^{-1/2} \left(\frac{\Sigma_{\text{SFR}}}{\text{M}_\odot \text{ yr}^{-1} \text{ kpc}^{-2}} \right) \quad (57)$$

and

$$T_c = 8.3 \times 10^7 \text{ K} \left(\frac{\epsilon_{\text{therm}}}{0.5} \right) \left(\frac{\beta}{2} \right)^{-1}. \quad (58)$$

I find that the high temperatures and low densities of starburst winds makes them extremely poor at free-free absorption. The free-free optical depth is tiny even at MHz frequencies:

$$\tau_{\text{ff}} \approx 4.2 \times 10^{-5} \left(\frac{\Sigma_{\text{SFR}}}{50 \text{ M}_\odot \text{ yr}^{-1} \text{ kpc}^{-2}} \right)^2 \left(\frac{\nu}{1 \text{ MHz}} \right)^{-2} \times \left(\frac{s}{100 \text{ pc}} \right) \quad (59)$$

assuming that $\bar{g}_{\text{ff}} = 20$ for MHz frequencies and $T \approx 10^8 \text{ K}$ plasmas. The turnover frequency is far below observability, since we are stuck in the Milky Way:

$$\nu_{\text{ff}} \approx 6.5 \text{ kHz} \left(\frac{\Sigma_{\text{SFR}}}{50 \text{ M}_\odot \text{ yr}^{-1} \text{ kpc}^{-2}} \right) \left(\frac{s}{100 \text{ pc}} \right)^{1/2} \quad (60)$$

The weakest starbursts have $\Sigma_{\text{SFR}} \approx 1 \text{ M}_\odot \text{ yr}^{-1} \text{ kpc}^{-2}$ and the star-formation rate surface density in M82 and NGC 253 is $\sim 50 \text{ M}_\odot \text{ yr}^{-1} \text{ kpc}^{-2}$, while Σ_{SFR} reaches $\sim 10^4 \text{ M}_\odot \text{ yr}^{-1} \text{ kpc}^{-2}$ in the most extreme starbursts. Therefore, the starburst wind introduces free-free absorption only at frequencies less than $\sim 0.1 - 1000 \text{ kHz}$, and is not important at the observable MHz radio frequencies fit by models.

5.2 Free-free absorption from cosmic ray-ionized molecular gas

Thompson, Quataert, & Murray (2005) have argued that cold molecular gas, instead of rarefied supernova-heated material, fills most of the volume of starbursts. This could happen if supernova remnants rapidly lose their

kinetic energy to radiative losses as they expand in a dense molecular medium, so that supernova-heated material fills only small isolated bubbles. Then the molecular gas will fill most of the starburst region, since the H II regions also have a small filling factor. Molecular gas is mostly neutral and dust extinction will rapidly extinguish any ultraviolet light. However, cosmic rays should provide a relatively high level of ionization through fairly large columns (Suchkov, Allen, & Heckman 1993; Papadopoulos 2010), though the details of CR diffusion in starbursts and their penetration into molecular material is poorly understood.

As I argued in Lacki (2012), the cosmic ray ionization rate in starburst galaxies, where the proton spectrum is relatively hard, is

$$\zeta_{\text{CR}} = \frac{\eta_{\text{ion}} L_{\text{CR}} m_H}{E_{\text{ion}} \dot{M}_H}. \quad (61)$$

In this equation, L_{CR} is the luminosity of injected cosmic rays, $E_{\text{ion}} \approx 30 \text{ eV}$ is the energy lost per cosmic ray ionization event (Cravens & Dalgarno 1978), M_H is the mass of gas in the galaxy, and $\eta_{\text{ion}} \approx 0.1$ is the fraction of cosmic ray power that goes into ionization. The injected cosmic ray luminosity is though to be approximately 10^{50} erg per supernova. For a Salpeter IMF extending from 0.1 to 100 M_\odot , the supernova rate is $\Gamma_{\text{SN}} = 0.0064 \text{ yr}^{-1} (\text{SFR}/\text{M}_\odot \text{ yr}^{-1})$. Therefore, the cosmic ray luminosity is approximately $L_{\text{CR}} \approx 2.0 \times 10^{40} \text{ erg s}^{-1} (\text{SFR}/\text{M}_\odot \text{ yr}^{-1})$.

Note that $\zeta_{\text{CR}} \propto \text{SFR}/M_H$, the inverse of the gas consumption time $\tau_{\text{gas}} \equiv M_H/\text{SFR}$. This time is equal to $\sim 20 \text{ Myr}$ for nuclear starbursts, so the ionization rate can be conveniently expressed in terms of τ_{gas} . The cosmic ray ionization rate is:

$$\zeta_{\text{CR}} \approx 1.8 \times 10^{-15} \text{ s}^{-1} \left(\frac{\tau_{\text{gas}}}{20 \text{ Myr}} \right)^{-1}. \quad (62)$$

The ionization fraction is set by the ratio of the gas density n_H and a characteristic density $n_{\text{ch}} \approx 1000 (\zeta_{\text{CR}}/10^{-17} \text{ s}^{-1})$:

$$x_e = 1 \times 10^{-7} \left(\frac{n_{\text{ch}}}{n_H} \right)^{1/2} \left[\left(1 + \frac{n_{\text{ch}}}{4n_H} \right)^{1/2} + \left(\frac{n_{\text{ch}}}{4n_H} \right)^{1/2} \right] \quad (63)$$

from McKee (1989). In the cosmic ray ionized gas of starbursts, $n_{\text{ch}} \gg n_H$ and $x_e \approx 10^{-7} (n_{\text{ch}}/n_H)$. Thus,

$$x_e \approx 3.5 \times 10^{-5} \left(\frac{\tau_{\text{gas}}}{20 \text{ Myr}} \right)^{-1} \left(\frac{n_H}{500 \text{ cm}^{-3}} \right)^{-1} \quad (64)$$

While the ionization fraction is low, free-free absorption is enhanced by two factors: molecular material is dense, so the density of electrons and ions is relatively high, and molecular gas is cold. The electrons and ions reach thermal equilibrium with the surrounding gas long before they recombine (e.g., McCall et al. 2002). Assuming typical starburst molecular gas temperatures of $\sim 100 \text{ K}$, I find free-free optical depths of

$$\tau_{\text{ff}} \approx 17 \left(\frac{\tau_{\text{gas}}}{20 \text{ Myr}} \right)^{-2} \left(\frac{T}{100 \text{ K}} \right)^{-3/2} \left(\frac{s}{100 \text{ pc}} \right) \left(\frac{\nu}{\text{MHz}} \right)^{-2} \quad (65)$$

assuming $n_e = n_i = x_e n_H$ and $\bar{g}_{\text{ff}} = 10$. The frequency of the free-free spectrum turnover is

⁶ The fraction of mass ejected by stellar winds and supernova that ends up in the wind; it can be greater than 1 if cold gas is swept up by the wind as it leaves the galaxy.

$$\nu_{\text{ff}} \approx 4.1 \text{ MHz} \left(\frac{\tau_{\text{gas}}}{20 \text{ Myr}} \right)^{-1} \left(\frac{T}{100 \text{ K}} \right)^{-3/4} \left(\frac{s}{100 \text{ pc}} \right)^{1/2} \quad (66)$$

If there really is a molecular medium with a high filling factor, and if it is cosmic ray ionized, it can terminate the low frequency radio spectrum of starbursts. With turnover frequencies of ~ 5 MHz, detecting it would be a challenging measurement, but one that is possible in principle, especially since the turnover is at higher frequency than that of the warm ionized medium in the Milky Way (and presumably the starburst's host galaxy), ~ 3 MHz. Thus, the presence or absence of a turnover at ~ 5 MHz can test whether cosmic ray ionized high filling-factor molecular gas really does exist in starbursts.

A factor that I have neglected is the highly supersonic turbulence present in starburst galaxies, which will generate large density fluctuations in the molecular gas, even without the existence of any other gas phases. However, if the ionization rate ζ_{CR} across the starburst is the same everywhere, the homogeneous approximation will give approximately the right results. This is because $x_e \propto n_H^{-1}$ and $\alpha_{\text{HII}} \propto x_e^2 n_H^2$: the free-free absorption coefficient does not vary with density. It is possible that the cosmic ray ionization rate decreases in high density regions because the cosmic rays are stopped by the gas (Lacki 2012), but these regions are those of low filling factor anyway.

5.3 The Razin effect

Free-free absorption is not the only process that cuts off the radio spectrum at low frequency. At low energies, the index of refraction of plasma suppresses the beaming of synchrotron radiation and causes it to fall off exponentially (Rybicki & Lightman 1979). The frequency where this Razin effect becomes important is

$$\nu_R = 185 \text{ kHz} \left(\frac{n_e}{1 \text{ cm}^{-3}} \right) \left(\frac{B}{100 \text{ } \mu\text{G}} \right)^{-1}, \quad (67)$$

from Schlickeiser (2002).

Suppose all the gas in the starburst, both ionized and neutral, has the same magnetic field. The Razin cutoff in the hot superwind phase is

$$\nu_R^{\text{wind}} = \begin{cases} 51 \text{ kHz} \left(\frac{\Sigma_{\text{SFR}}}{50 \text{ M}_{\odot} \text{ yr}^{-1}} \right) \left(\frac{B}{200 \text{ } \mu\text{G}} \right)^{-1} \\ 340 \text{ kHz} \left(\frac{\Sigma_{\text{SFR}}}{10^4 \text{ M}_{\odot} \text{ yr}^{-1}} \right) \left(\frac{B}{6 \text{ mG}} \right)^{-1} \end{cases} \quad (68)$$

where the upper values are scaled to values expected in M82 and the lower values are scaled to values expected in Arp 220's radio nuclei. In fact, B and Σ_{SFR} are likely to depend on each other. The existence of the linear far-infrared radio correlation of galaxies constrains magnetic field strengths to be

$$B_{\text{FRC}} \approx 67 \text{ } \mu\text{G} \sqrt{\Sigma_{\text{SFR}} / (\text{M}_{\odot} \text{ yr}^{-1} \text{ kpc}^{-2})} \quad (69)$$

from Lacki et al. (2010), after using the Kennicutt (1998) Schmidt law to convert between gas surface density and star-formation surface density. Applying this value of B to equation 68, the Razin cutoff is

$$\nu_R^{\text{wind}} = 21 \text{ kHz} \left(\frac{\Sigma_{\text{SFR}}}{50 \text{ M}_{\odot} \text{ yr}^{-1}} \right)^{1/2}, \quad (70)$$

varying between 3 and 300 kHz for starbursts with Σ_{SFR} between 1 and $10^4 \text{ M}_{\odot} \text{ yr}^{-1} \text{ kpc}^{-2}$.

If starbursts are instead filled with cosmic ray ionized gas, the low electron density ($n_e = x_e n_H$) of these regions imply still lower Razin cutoffs:

$$\nu_R^{\text{mol}} = \begin{cases} 1.6 \text{ kHz} \left(\frac{\tau_{\text{gas}}}{20 \text{ Myr}} \right)^{-1} \left(\frac{B}{200 \text{ } \mu\text{G}} \right)^{-1} \\ 54 \text{ Hz} \left(\frac{\tau_{\text{gas}}}{20 \text{ Myr}} \right)^{-1} \left(\frac{B}{6 \text{ mG}} \right)^{-1} \end{cases} \quad (71)$$

In high density molecular regions of material, the ionization rate is lower, and Zeeman splitting measurements indicate the magnetic field may be even higher (Robishaw, Quataert, & Heiles 2008), so the Razin effect could be even less important.

Where the Razin effect might be important is in H II regions, which are fully ionized and high density:

$$\nu_R^{\text{HII}} = \begin{cases} 46 \text{ MHz} \left(\frac{n_H}{500 \text{ cm}^{-3}} \right) \left(\frac{B}{200 \text{ } \mu\text{G}} \right)^{-1} \\ 31 \text{ MHz} \left(\frac{n_H}{10000 \text{ cm}^{-3}} \right) \left(\frac{B}{6 \text{ mG}} \right)^{-1} \end{cases} \quad (72)$$

Within these regions, we see that free-free absorption – which turns H II regions opaque at GHz frequencies – is more important than the Razin effect.

I conclude that the Razin effect is not observable in starburst galaxies.

5.4 Synchrotron self-absorption

Both free-free absorption and Razin cutoff depend on the density distribution of ionized matter, something which is not entirely certain in starburst galaxies. However, because we observe synchrotron emission from starburst galaxies, there must also be synchrotron self-absorption in them as well.

The maximum brightness temperature of a synchrotron source, as limited by synchrotron self-absorption, is

$$T_{\text{max}} \approx 3 \times 10^{12} \text{ K} \left(\frac{\nu}{\text{GHz}} \right)^{1/2} \left(\frac{B}{100 \text{ } \mu\text{G}} \right)^{-1/2} \quad (73)$$

from Begelman, Blandford, & Rees (1984).

For resolved starbursts with an observed low frequency radio spectrum, it is possible to simply fit a model to the radio spectrum and see when, if ever, the brightness temperature T_b is greater than T_{max} . In general, though we expect starbursts to lie on the far-infrared radio correlation, with $\nu L_{\nu}(1 \text{ GHz}) = 10^{-6} L_{\text{TIR}} = 5630 L_{\odot} (\text{SFR}/\text{M}_{\odot} \text{ yr}^{-1})$ (Kennicutt 1998; Yun, Reddy, & Condon 2001). Ignoring geometrical factors, the starburst can be thought of as a sphere with radius R_{SB} , so that the intensity is $I_{\nu} = L_{\nu}/(4\pi^2 R_{\text{SB}}^2)$. Likewise, the star-formation surface density is $\Sigma_{\text{SFR}} = \text{SFR}/(\pi R_{\text{SB}}^2)$. Finally, since we are in the Rayleigh-Jeans limit, $T_b = c^2 I_{\nu}/(2\nu^2 k)$. Putting all these formulas together, I find that the FIR-radio correlation implies

$$T_b(1 \text{ GHz}) \approx 600 \text{ K} \left(\frac{\Sigma_{\text{SFR}}}{\text{M}_{\odot} \text{ yr}^{-1} \text{ kpc}^{-2}} \right). \quad (74)$$

Now we need to extrapolate this down to low radio frequencies. The simplest assumption is that the radio spectral index is constant and equal to -0.7 . Then by setting $T_b = T_b(1 \text{ GHz})(\nu/\text{GHz})^{-2.7}$, using eqn. 69 for B , and equating eqns. 73 and 74, I find the synchrotron self-absorption turnover for M82 is at:

$$\nu_{\text{SSA}} = 3.5 \text{ MHz} \left(\frac{\Sigma_{\text{SFR}}}{50 \text{ M}_{\odot} \text{ yr}^{-1} \text{ kpc}^{-2}} \right)^{0.31} \left(\frac{B}{200 \mu\text{G}} \right)^{0.16} \quad (75)$$

Plugging in the B field strength from the far-infrared radio correlation (eqn. 69), I find

$$\nu_{\text{SSA}} = 4.0 \text{ MHz} \left(\frac{\Sigma_{\text{SFR}}}{50 \text{ M}_{\odot} \text{ yr}^{-1} \text{ kpc}^{-2}} \right)^{0.39}. \quad (76)$$

For starbursts with $1 \leq \Sigma_{\text{SFR}}/(\text{M}_{\odot} \text{ yr}^{-1} \text{ kpc}^{-2}) \leq 10^4$, $\nu_{\text{SSA}} \approx 0.9 - 30 \text{ MHz}$. This result is conservative, though, since the radio spectra display both partially-covered free-free absorption and intrinsic spectral curvature. Moreover, starburst radio spectra tend to be somewhat flatter than $\alpha = 0.7$.

I can use my model fit to the spectrum of M82 to account for these effects. Taking $\mathcal{B} = -\alpha = -0.6$ and $\mathcal{C} = -0.1$, I combine eqns. 74 and 73 to find

$$\log_{10} \left(\frac{\nu_{\text{SSA}}}{\text{GHz}} \right) = -15.5 + 5 \sqrt{5.69 + 0.4 \log_{10}(f \Sigma_{\text{SFR}}^{5/4})}, \quad (77)$$

where f is the fraction of flux transmitted by free-free absorbing H II regions at low frequencies. When $f = 1$, I find synchrotron self-absorption turnovers at $0.3 - 20 \text{ MHz}$ for $1 \leq \Sigma_{\text{SFR}}/(\text{M}_{\odot} \text{ yr}^{-1} \text{ kpc}^{-2}) \leq 10^4$, with a turnover at 2 MHz for M82; when $f = 0.5$, the synchrotron turnovers for starbursts are nearly the same ($0.2 - 20 \text{ MHz}$; 1.5 MHz for M82).

The synchrotron self-absorption cutoffs are higher than the free-free absorption cutoffs for the starburst wind. Since they are in the MHz range, they may be observable, especially for Arp 220 with a frequency cutoff at $\sim 5 - 20 \text{ MHz}$. A measured synchrotron turnover frequency would tell us what the magnetic field strength in starburst galaxies really is.

The Razin effect actually suppresses not only synchrotron emission, but synchrotron absorption (Crusius & Schlickeiser 1988). Below the Razin cutoff, there can even be negative absorption and stimulated emission (Crusius & Schlickeiser 1988). However, the Razin cutoff is at much lower frequencies than the synchrotron self-absorption turnover. Furthermore, when the Razin effect does operate, there is still a cutoff in the observed synchrotron radio emission, so either way the radio spectrum ends.

5.5 Summary

Of the processes I considered, the most likely to produce a true low frequency turnover in starburst radio spectra is synchrotron self-absorption, which should be important only below $\sim 20 \text{ MHz}$ even for Arp 220-like compact starbursts. If there is a volume-filling molecular medium that is ionized by cosmic rays, it may also cause a free-free absorption turnover, but only below $\sim 5 \text{ MHz}$. The volume-filling

10^8 K superwind is too hot and rarefied to produce appreciable free-free absorption at observable frequencies. Nor is the Razin effect important.

It is in principle possible that there are diffuse ionized phases that I do not consider, perhaps like the warm ionized medium in the Milky Way. Such phases could be constrained by the amount of free-free absorption. In fact, the Milky Way's own warm ionized medium will prevent observations below a few MHz, and it is likely the warm ionized medium in starbursts' surrounding host galaxies will do the same, especially if they are viewed edge-on. However, given our current understanding of the phases likely to fill most of the starbursts, it appears that starbursts are largely transparent to $\lesssim 20 \text{ MHz}$.

6 CONCLUSIONS

With the renewed interest in low frequency radio astronomy, it is time for a better theoretical understanding of the low frequency radio spectra of starburst galaxies. Previous models of the emission at these frequencies, if they considered free-free absorption at all, predicted that starbursts are opaque below a GHz. This was because they used the uniform slab model, essentially assuming that ionized gas evenly pervaded the starburst. Most of the ionized gas mass is not truly diffuse in starbursts, but instead resides in discrete H II regions. In fact discrete H II regions are responsible for much of the free-free absorption in the Galactic Centre (Brogan et al. 2003; Nord et al. 2006), a region in some ways analogous to starbursts but close enough to be easily resolved (Crocker et al. 2011). A low frequency map of M82 also indicates discrete H II regions as the source of free-free absorption (Wills et al. 1997). If the H II regions are uniformly distributed throughout the starburst, they contribute to an effective absorption coefficient which should be used in the uniform slab formula. This coefficient does not approach infinity at low frequencies. H II regions only partially cover the starburst, leaving sightlines where the emission is unobscured. Furthermore, the H II regions are usually some way in from the surface of the starburst, so there is unobscured synchrotron emitting material on a sightline in front of the nearest H II region.

I showed how to calculate this effective absorption coefficient in the limit that the H II regions do not fill most of the starburst, which is usually true. The calculation ultimately reduces down to the density of the H II regions multiplied by the cross section of each to absorb background radio waves. I applied the calculations to the radio spectrum of M82. I find that models with discrete H II regions, around either individual O stars or Super Star Clusters, are able to reproduce the radio spectrum reasonably well, even at frequencies down to 23 MHz (see Figures 5, 6, and 7).

The models I presented in the paper were relatively simple, assuming that H II regions are characterized by a single temperature and density. However, if the temperature and density distribution is known through other means, such as radio recombination lines, it is straightforward to integrate up the cross sections and calculate the effective absorption coefficient. A more important flaw in the approach described here is that I assume that H II regions are uniformly dense Strömberg spheres. However, dust absorption affects both

the amount of ionizing photons available to produce H II regions (Petrosian et al. 1972), and the structure of H II regions (Draine 2011b). Since my models suggest a low amount of free-free emission, which could mean that dust is absorbing ionizing photons, it is important that these effects be studied.

This work implies that starbursts are in fact fairly bright at low frequencies. I considered whether any other absorption process could cause a turnover in the radio spectrum. I found that free-free absorption from the volume-filling superwind phase of starbursts, and the Razin effect, are negligible down to kHz frequencies in starbursts. Synchrotron self-absorption should become important at frequencies of a few MHz. If there is a volume-filling phase of cold molecular gas, ionized by cosmic rays, it can also cause free-free absorption at a few MHz.

ACKNOWLEDGMENTS

BCL was supported by a Jansky Fellowship from the National Radio Astronomy Observatory. The National Radio Astronomy Observatory is operated by Associated Universities, Inc., under cooperative agreement with the National Science Foundation. I am grateful to Rainer Beck and Diego Torres for comments on this research.

REFERENCES

- Alexander, J. K., Brown, L. W., Clark, T. A., Stone, R. G., & Weber, R. R. 1969, *ApJL*, 157, L163
- Anantharamaiah, K. R., Zhao, J.-H., Goss, W. M., & Viallefond, F. 1993, *ApJ*, 419, 585
- Artyukh, V. S., Dagkesamanskii, V. V., Vitkevich, R. D., & Kozhukhov, V. N. 1969, *Soviet Ast.*, 12, 567
- Baldwin, J. E., Boysen, R. C., Hales, S. E. G., Jennings, J. E., Waggett, P. C., Warner, P. J., Wilson, D. M. A. 1985, *MNRAS*, 217, 717
- Basu, A., Mitra, D., Wadadekar, Y., & Ishwara-Chandra, C. H. 2012, *MNRAS*, 419, 1136
- Begelman, M. C., Blandford, R. D., & Rees, M. J. 1984, *Reviews of Modern Physics*, 56, 255
- Brogan, C. L., Nord, M., Kassim, N., Lazio, J., & Anantharamaiah, K. 2003, *Astronomische Nachrichten Supplement*, 324, 17
- Carilli, C. L. 1996, *A&A*, 305, 402
- Chevalier, R. A., & Clegg, A. W. 1985, *Nature*, 317, 44
- Clemens, M. S., Vega, O., Bressan, A., Granato, G. L., Silva, L., Panuzzo, P. 2008, *A&A*, 477, 95
- Clemens, M. S., Scaife, A., Vega, O., & Bressan, A. 2010, *MNRAS*, 405, 887
- Cohen, A. S., Lane, W. M., Cotton, W. D., Kassim, N. E., Lazio, T. J. W., Perley, R. A., Condon, J. J., Erickson, W. C. 2007, *AJ*, 134, 1245
- Condon, J. J., Huang, Z.-P., Yin, Q. F., & Thuan, T. X. 1991, *ApJ*, 378, 65
- Condon, J. J. 1992, *ARA&A*, 30, 575
- Cravens, T. E., & Dalgarno, A. 1978, *ApJ*, 219, 750
- Crocker, R. M., Jones, D. I., Aharonian, F., Law, C. J., Melia, F., Oka, T., & Ott, J. 2011, *MNRAS*, 413, 763
- Crusius, A., & Schlickeiser, R. 1988, *A&A*, 196, 327
- de Cea del Pozo, E., Torres, D. F., & Rodriguez Marrero, A. Y. 2009, *ApJ*, 698, 1054
- Domingo-Santamaría, E. & Torres, D. F. 2005, *A&A*, 444, 403
- Draine, B. T. 2011a, *Physics of the Interstellar and Inter-galactic Medium* (Princeton: Princeton University Press)
- Draine, B. T. 2011b, *ApJ*, 732, 100
- Ellingson, S. W., Clarke, T. E., Cohen, A., Craig, J., Kassim, N. E., Pihlstrom, Y., Rickard, L. J., Taylor, G. B. 2009, *IEEE Proceedings*, 97, 1421
- Fleishman, G. D., & Tokarev, Y. V. 1995, *A&A*, 293, 565
- Förster Schreiber, N. M., Genzel, R., Lutz, D., & Sternberg, A. 2003, *ApJ*, 599, 193
- Freedman, W. L., & Madore, B. F. 1988, *ApJL*, 332, L63
- Freedman, W. L., et al. 1994, *ApJ*, 427, 628
- Goetz, M., Downes, D., Greve, A., & McKeith, C. D. 1990, *A&A*, 240, 52
- Hales, S. E. G., Mayer, C. J., Warner, P. J., & Baldwin, J. E. 1991, *MNRAS*, 251, 46
- Heckman, T. M., Armus, L., & Miley, G. K. 1990, *ApJS*, 74, 833
- Hummel, E. 1991, *A&A*, 251, 442
- Israel, F. P., & Mahoney, M. J. 1990, *ApJ*, 352, 30
- Kassim, N. E., Lazio, T. J. W., Erickson, W. C., et al. 2007, *ApJS*, 172, 686
- Kellermann, K. I., Pauliny-Toth, I. I. K., & Williams, P. J. S. 1969, *ApJ*, 157, 1
- Kennicutt, R. C. 1998, *ApJ*, 498, 541
- Kepley, A. A., Chomiuk, L., Johnson, K. E., Goss, W. M., Balser, D. S., Pisano, D. J. 2011, *ApJL*, 739, L24
- Klein, U., Wielebinski, R., & Morsi, H. W. 1988, *A&A*, 190, 41
- Lacki, B. C., Thompson, T. A., & Quataert, E. 2010, *ApJ*, 717, 1
- Lacki, B. C. 2012, *arXiv:1204.2580*
- Laing, R. A., & Peacock, J. A. 1980, *MNRAS*, 190, 903
- Leitherer, C., Schaerer, D., Goldader, J. D., et al. 1999, *ApJS*, 123, 3
- Leroy, A. K., Evans, A. S., Momjian, E., et al. 2011, *ApJL*, 739, L25
- Lord, S. D., Hollenbach, D. J., Haas, M. R., Rubin, R. H., Colgan, S. W. J., Erickson, E. F. 1996, *ApJ*, 465, 703
- McCall, B. J., Hinkle, K. H., Geballe, T. R., et al. 2002, *ApJ*, 567, 391
- McCraday, N., & Graham, J. R. 2007, *ApJ*, 663, 844
- McDonald, A. R., Muxlow, T. W. B., Wills, K. A., Pedlar, A., & Beswick, R. J. 2002, *MNRAS*, 334, 912
- McKee, C. F., & Ostriker, J. P. 1977, *ApJ*, 218, 148
- McKee, C. F. 1989, *ApJ*, 345, 782
- Melo, V. P., Muñoz-Tuñón, C., Maíz-Apellániz, J., & Tenorio-Tagle, G. 2005, *ApJ*, 619, 270
- Meurer, G. R., Heckman, T. M., Leitherer, C., Kinney, A., Robert, C., Garnett, D. R. 1995, *AJ*, 110, 2665
- Murphy, E. J. 2009, *ApJ*, 706, 482
- Niklas, S., Klein, U., & Wielebinski, R. 1997, *A&A*, 322, 19
- Nord, M. E., Henning, P. A., Rand, R. J., Lazio, T. J. W., & Kassim, N. E. 2006, *AJ*, 132, 242
- O’Connell, R. W., Gallagher, J. S., III, Hunter, D. A., & Colley, W. N. 1995, *ApJL*, 446, L1
- Papadopoulos, P. P. 2010, *ApJ*, 720, 226
- Perley, R. A., Chandler, C. J., Butler, B. J., & Wrobel,

- J. M. 2011, *ApJL*, 739, L1
- Persic, M., Rephaeli, Y., & Arieli, Y. 2008, *A&A*, 486, 143
- Peterson, J. D., & Webber, W. R. 2002, *ApJ*, 575, 217
- Petrosian, V., Silk, J., & Field, G. B. 1972, *ApJL*, 177, L69
- Puxley, P. J., Brand, P. W. J. L., Moore, T. J. T., Mountain, C. M., Nakai, N., Yamashita, T. 1989, *ApJ*, 345, 163
- Rengarajan, T. N. 2005, *Proc. 29th Int. Cosmic Ray Conf. (Pune)*, 3.
- Rephaeli, Y., Arieli, Y., & Persic, M. 2010, *MNRAS*, 401, 473
- Robishaw, T., Quataert, E., & Heiles, C. 2008, *ApJ*, 680, 981
- Rodriguez-Rico, C. A., Viallefond, F., Zhao, J.-H., Goss, W. M., & Anantharamaiah, K. R. 2004, *ApJ*, 616, 783
- Rodríguez-Rico, C. A., Goss, W. M., Viallefond, F., Zhao, J.-H., Gómez, Y., Anantharamaiah, K. R. 2005, *ApJ*, 633, 198
- Roger, R. S., Costain, C. H., & Stewart, D. I. 1986, *A&AS*, 65, 485
- Rybicki, G. B. & Lightman, A. P. 1979, *Radiative Processes in Astrophysics*, (New York: Wiley-VCH)
- Sakai, S., & Madore, B. F. 1999, *ApJ*, 526, 599
- Sanders, D. B., Mazzarella, J. M., Kim, D.-C., Surace, J. A., & Soifer, B. T. 2003, *AJ*, 126, 1607
- Schlickeiser, R. 2002, *Cosmic Ray Astrophysics*, (New York: Springer).
- Smith, L. J., Westmoquette, M. S., Gallagher, J. S., O'Connell, R. W., Rosario, D. J., de Grijs, R. 2006, *MNRAS*, 370, 513
- Sopp, H. M., & Alexander, P. 1989, *ApSS*, 157, 287
- Sopp, H. M., & Alexander, P. 1991, *MNRAS*, 251, 112
- Strickland, D. K., & Stevens, I. R. 2000, *MNRAS*, 314, 511
- Strickland, D. K., & Heckman, T. M. 2007, *ApJ*, 658, 258
- Strickland, D. K., & Heckman, T. M. 2009, *ApJ*, 697, 2030
- Suchkov, A., Allen, R. J., & Heckman, T. M. 1993, *ApJ*, 413, 542
- Thompson, T. A., Quataert, E., & Murray, N. 2005, *ApJ*, 630, 167
- Thompson, T. A., Quataert, E., Waxman, E., Murray, N., & Martin, C. L. 2006, *ApJ*, 645, 186
- Torres, D. F. 2004, *ApJ*, 617, 966
- Torres, D. F., Cillis, A., Lacki, B., & Rephaeli, Y. 2012, *MNRAS*, 423, 822
- Westmoquette, M. S., Smith, L. J., Gallagher, J. S., III, O'Connell, R. W., Rosario, D. J., de Grijs, R. 2007, *ApJ*, 671, 358
- Williams, P. K. G., & Bower, G. C. 2010, *ApJ*, 710, 1462
- Wills, K. A., Pedlar, A., Muxlow, T. W. B., & Wilkinson, P. N. 1997, *MNRAS*, 291, 517
- Yun, M. S., Reddy, N. A., & Condon, J. J. 2001, *ApJ*, 554, 803
- Zhao, J.-H., Anantharamaiah, K. R., Goss, W. M., & Viallefond, F. 1996, *ApJ*, 472, 54